The parietal operculum preferentially encodes heat pain and not salience

Björn Horing, Christian Sprenger, Christian Büchel

Björn Horing, Ph.D. (corresponding author)
Affective Neuroscience Group
Department of Systems Neuroscience
University Medical Center Hamburg-Eppendorf
email b.horing@uke.de
phone +49 040 7410 - 57890

Christian Sprenger, M.D.
Affective Neuroscience Group
Department of Systems Neuroscience
University Medical Center Hamburg-Eppendorf

Christian Büchel, M.D.
Affective Neuroscience Group
Department of Systems Neuroscience
University Medical Center Hamburg-Eppendorf

Abstract

Substantial controversy exists as to which part of brain activity is genuinely attributable to pain-related percepts, and which activity is due to general aspects of sensory stimulation, such as its salience, or the accompanying arousal. The challenge posed by this question rests largely in the fact that pain per se exhibits highly intense but unspecific characteristics. These therefore should be matched by potential control conditions. Here, we used a unique combination of functional magnetic resonance imaging, behavioral and autonomic measures to address this longstanding debate in pain research.

Subjects rated perceived intensity in a sequence alternating between heat and sound stimuli. Neuronal activity was monitored using fMRI. Either modality was presented in six different intensities, three of which lay above the pain threshold (for heat) or the unpleasantness threshold (for sound). We performed our analysis on 26 volunteers in which psychophysiological responses (as per skin conductance responses) did not differ between the two stimulus modalities. Having thus ascertained a comparable amount of stimulation-related but unspecific activation, we analyzed stimulus response functions after painful stimulation, and contrasted them with those of the matched acoustic control condition. Furthermore, analysis of fMRI data was performed on the brain surface to circumvent blurring issues stemming from the close proximity of several regions of interest located in heavily folded cortical areas. We focused our analyses on insular and periinsular regions which are strongly involved in processing of painful stimuli. We employed an axiomatic approach to determine areas showing higher activation in painful compared to non-painful heat, and at the same time showing a steeper stimulus response function for painful heat as compared to unpleasant sound. Intriguingly, an area in the posterior parietal operculum emerged whose response showed a pain preference after satisfying all axiomatic constraints.

This result has important implications for the interpretation of functional imaging findings in pain research, as it clearly demonstrates that there are areas whose activity following painful stimulation

is not due to general attributes or results of sensory stimulation, such as salience or arousal. Conversely, several areas did not conform to the formulated axioms to rule out general factors as explanations.

Introduction

Pain is a multidimensional experience, including sensory-discriminative, affective-motivational, cognitive-evaluative as well as motor components [1], and is defined as “an unpleasant sensory and emotional experience associated with actual or potential tissue damage, or described in terms of such damage” [2]. Following the advent of brain imaging, recurring patterns of brain activity following painful stimuli were identified, comprising primary and secondary somatosensory cortices, cingulate cortices, as well as the insular subregions, among other structures [3,4].

This activity has frequently been attributed to pain per se. However, precisely because pain is a composite sensation, the utility of assigning it a fixed set of brain areas as a simplistic “pain matrix” has been contested [3,4]. The notion that some of the observed activation may or may not be exclusively pain-related has eventually led to a direct challenge to the concept of such a matrix [5,6]. These studies have provided evidence that in many cortical regions, activation is observed following both painful and non-painful (such as tactile or auditory) stimuli. In fact, general processes have long been posited as alternative explanations – for example, stimulus anticipation [7], magnitude estimation [8], or stimulus salience [5]. These contributions have led to lively controversy [9–12], and a large number of studies continues to address related issues using multiple modalities, and both univariate and multivariate approaches [13–18]. The status of the challenge to the “pain matrix” concept has recently been revisited [19]. This review reemphasized that great care should be taken experimentally to match non-painful control modalities, which has frequently been neglected in previous studies.

In addition to the question of general, modality-independent stimulus characteristics, many experiments have relied on the use of single stimulus intensities to characterize neuronal responses, when using painful stimulation and compared these responses to a non-painful control condition. However, such approaches disregard the possibility of modality-specific baseline activation, further compounding the issue to properly account for nonspecific activation [12]. A possible solution is to

employ multiple stimulus intensities, which allows for the characterization of modality-specific stimulus-response functions [20–22], and a comparison of these between modalities.

Here, we address these issues, and present a novel approach that allows to directly test whether there are cortical regions that can be viewed as “salience detectors”, or show preferential pain processing. Please note that the term “salience” here and in the following does not refer to any narrowly defined physiological or cognitive construct, but is instead meant as generic term referencing the unspecific, modality-independent results of sensory stimulation. We employed heat and sound as stimulus modalities. Stimuli were presented in alternating modalities in a within-subjects design. Of each modality, we used six graded intensities – three below and three above the pain and unpleasantness threshold, respectively. This allowed us to determine stimulus-response functions of physical intensities or their percepts, and relate those to neuronal activity [20–23]. Importantly, auditory and thermal intensities were calibrated to match using an objective autonomic measure (skin conductance responses; SCR) [24].

We paid particular attention to insular and periinsular regions, especially the posterior insula and the parietal operculum (the secondary somatosensory cortex), all of which have been reported as cortical areas that are active early after painful stimulation [4,11,25–27].

To define areas as preferentially pain-processing, our analyses followed an axiomatic approach which posits several logical conditions to be met to make a valid inference (see [28], for a similar approach in pain avoidance). Within this rigorous approach, we formulated the following set of conditions to preclude the possibility that activity in an area could be explained by salience alone: The effect of painful stimulation should be larger than that of non-painful heat (axiom 1); the effect of painful stimulation should be larger than that of (salience-matched) unpleasant sound (axiom 2); the relationship of ratings and BOLD should be stronger for painful heat than for non-painful heat (axiom 3); the positive relationship of pain ratings and BOLD responses should be stronger for painful heat than for (salience-matched) unpleasant sound (axiom 4).

Results

Heat stimuli were presented using a CHEPS thermode, sounds were 1kHz beeps presented binaurally via headphones. For a brief overview, see Fig 1. Details are provided in the Materials and Methods section.

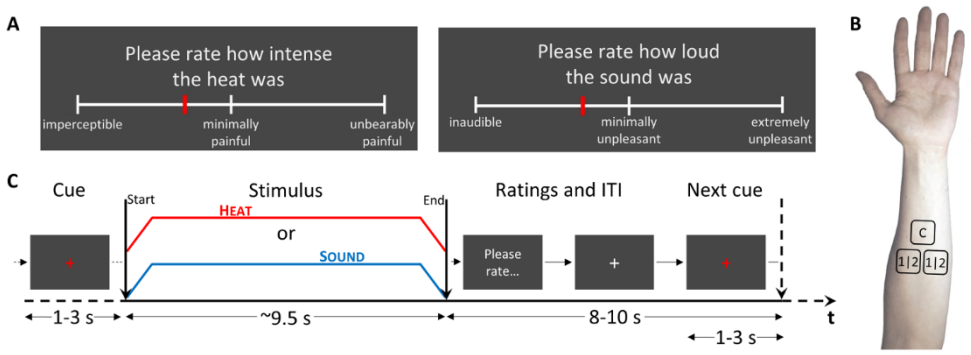

Fig 1. Experimental procedures. **A.** Visual analogue scales (VAS) for rating heat (left) and sound stimuli (right). The midpoint signifies the pain threshold, corresponding to a score of 0 in a conventional VAS. **B.** Thermode arrangement on a subject's forearm. Patch C was used for calibration, patches 1|2 were used in counterbalanced fashion for experimental sessions 1 and 2. **C.** Protocol by time. A visual cue (white fixation cross turning red) announced the upcoming stimulus (either heat or sound) and stayed visible throughout stimulation, which was 8 seconds at plateau (roughly 9.5 seconds all in all, depending on calibration). Subjects were then prompted to rate the stimulus. After rating, the white fixation cross reappeared, to turn red again for the next cue. Stimulus modalities were always alternating.

Sample

A core prerequisite of our analysis strategy was that both modalities (heat and sound) were matched with respect to salience. Although previous studies based estimates of general stimulus characteristics on ratings, such as salience ratings [5] or perceived intensity ratings [13,15], this can be problematic when comparing modalities, due to differential scaling of responses. We therefore selected skin conductance responses (SCR) as an objective readout parameter linked to modality-

124 independent processes such as emotion, cognition, or attention [24,29–31]. Consequently, our
125 approach is based on comparable SCR for sound and heat stimuli. This necessitated the selection of
126 suitable subjects and experimental sessions that fulfilled this criterion (see Materials and Methods).
127 Analysis included N=26 subjects (50% female, mean age±SD 25.8±3.6; see S1 Tab for more detailed
128 sample characteristics).

129

130 *Skin conductance results*

131 As intended by stimulus matching, no significant difference between modalities prevailed (p=0.177)
132 (random intercept model; Fig 2). SCR increased by intensity (t(308)=7.797, p=1e-13). There was no
133 interaction between intensity and modality (p=0.514).

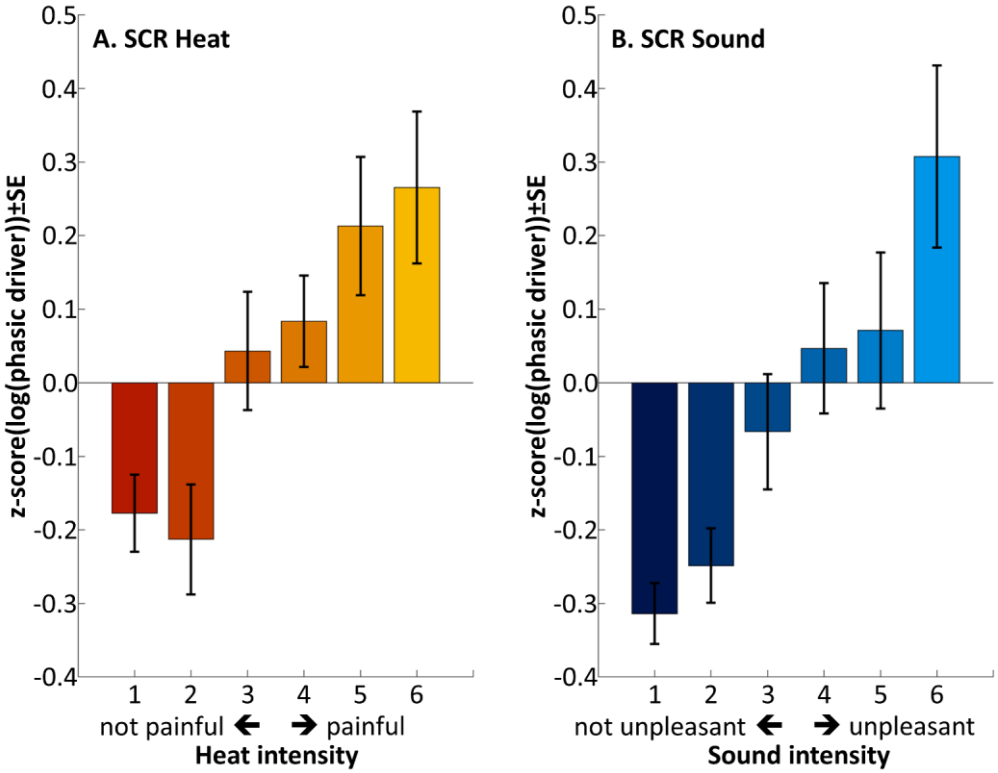

134

135 **Fig 2.** Skin conductance responses following heat (**A**) and sound stimuli (**B**). The pain and unpleasantness
136 thresholds were located between intensities 3 and 4, as per calibration. Individual data is shown in S1 Fig and
137 S2 Fig.

Stimulus calibration results

Mean heat pain threshold was at 43.3±1.1°C (range 40.5 to 45.4) and corresponded to 50 points on a 0 to 100 point visual analogue scale (VAS). Temperatures for stimulus intensities below and above pain threshold, corresponding to VAS targets of 25, 35, 45, 55, 65 and 75, were 41.7±1.4°C, 42.3±1.2°C, 43.0±1.1°C, 43.7±1.0°C, 44.3±1.0°C and 45.0±1.1°C, respectively. Mean unpleasantness threshold was at 83.9±7.0dBA (range 66.7-99.8). For additional details on heat and sound calibration, see Materials and Methods, and S2 Tab.

Behavioral results

The analysis of subjective ratings of sound and heat stimuli revealed a significant effect of modality ($t(320)=7.820$, $p=8e-14$; average sound rated estimate±SE 13.3±1.7 VAS points higher than average heat) (random intercept model; Fig 3) and a main effect of intensity ($t(320)=42.014$, $p=2e-16$; 11.8±0.3 VAS points per intensity step). The interaction between intensity and modality was also significant ($t(320)=-4.1529$, $p=4e-5$; 2.3±0.6 VAS points shallower slope in sound, per intensity step).

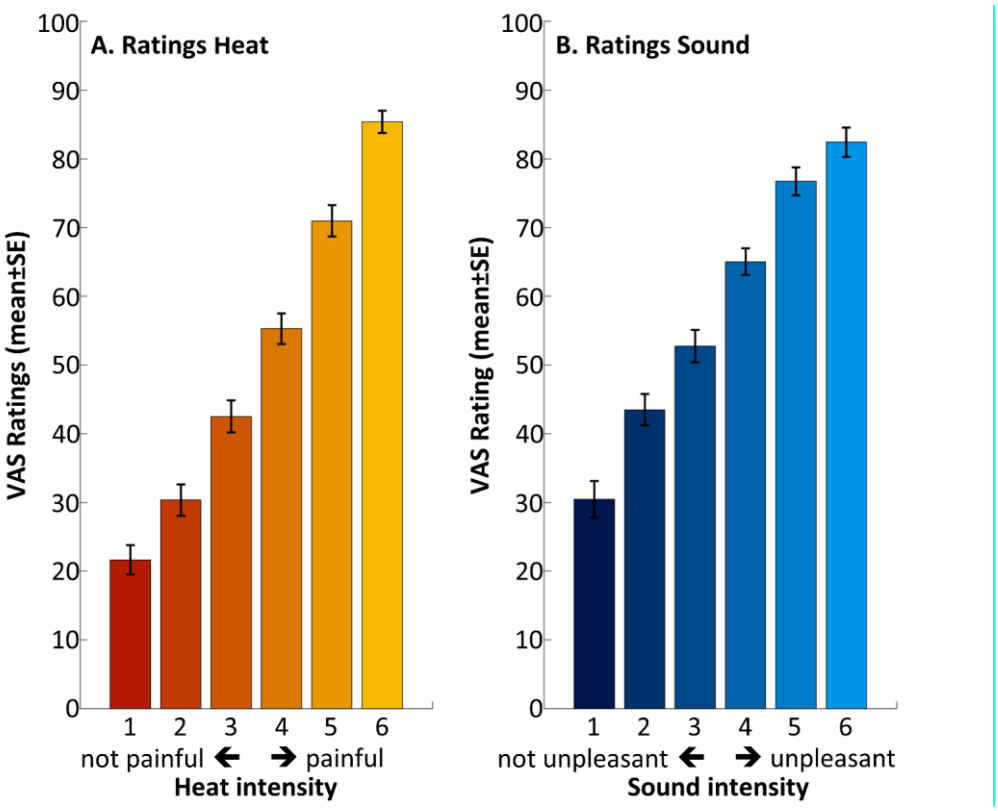

Fig 3. Behavioral ratings following heat (**A**) and sound stimuli (**B**). The pain and unpleasantness thresholds were located between intensities 3 and 4, as per calibration. Individual data is shown in S3 Fig.

Imaging results

For either modality, a mask was used that was obtained from main effect activations a) larger than the respective comparator modality and b) larger than baseline (S4A Fig; see Materials and Methods for details). The same mask was applied to all contrasts reported in the following, with the exception of conjunction analyses, which were performed without mask. Application of the masks constrains the analyses to areas consistently activated during stimulation of the respective modality. Within the same general area, figures with imaging results use consecutively numbered subscripts (for example, PO_1 always references the first significant peak described in the parietal operculum).

168 **Main effects of modality**

169 To test for intermodal differences, we contrasted the main effects for heat and sound (Fig 4).

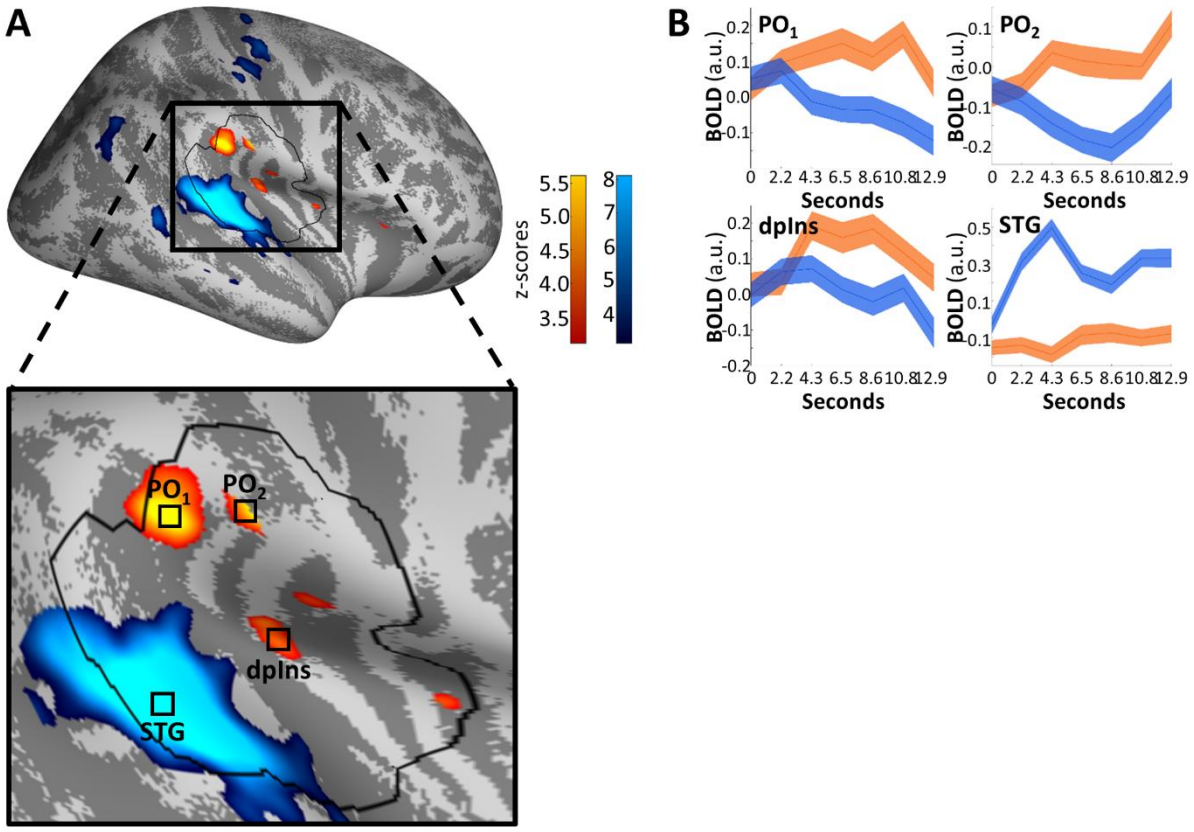

170

171 **Fig 4.** Differential effects of heat (orange) and sound (blue). Significant differences were found in the parietal
172 operculum (PO_1 and the more anterior PO_2) and dorsal posterior insula ($dpIns_1$) for heat; in the superior
173 temporal gyrus (STG_1) and Heschl's gyri for sound. **A.** Activations are thresholded at p(uncorrected)<0.001 and
174 overlaid on an average brain surface for display purposes. The black line delineates the region of interest used
175 for correction for multiple comparisons. See S5 Fig for peak locations in brain volume slices. **B.** Poststimulus
176 plots of fMRI activation over all stimulus intensities (mean±SE). Subplots PO_1, PO_2 and $dpIns_1$ show that heat-
177 related activation (orange) dominates in the analyzed time frames (seconds 2.2 through 10.8, see Materials and
178 Methods), while subplot STG_1 shows increased sound activation (blue).

179

180 The parietal operculum (secondary somatosensory cortex; peak MNI coordinates x=51, y=-30, z=28,
181 Z=5.62, p(corrected)=1e-05; second peak at x=59, y=-23, z=25, Z=5.221, p(corrected)=1e-04) and

182 dorsal posterior insula (x=40, y=-21, z=19, Z=4.175, p(corrected)=0.012) showed stronger activation
183 for heat as compared to sound. Conversely, Heschl's gyri (primary auditory cortex; x=64, y=-24, z=7,
184 Z=Inf, p(corrected)=4e-16) showed stronger activation for sound stimuli.

185 Of note, areas activated by either modality show no overlap, as determined via conjunction analyses,
186 even at a liberal threshold of p(uncorrected)<0.001, of contrasts of heat or sound larger than
187 baseline activation. The conjunction analysis did not use any masking; regardless, it did not yield
188 significant results.

189

190 **Parametric modulation by stimulus intensity**

191 Irrespective of modality, main effects can be confounded by unspecific effects associated with the
192 generic occurrence of an external stimulus, such as orientation and response preparation. Therefore,
193 we performed an analysis investigating stimulus response functions (SRFs), i.e., testing for stronger
194 BOLD responses for higher stimulus intensities.

195 We contrasted both modalities to identify areas with diverging SRFs within those areas showing a
196 main effect of either modality, as determined above. For heat, we identified activity in the parietal
197 operculum (x=57, y=-30, z=31, Z=3.999, p(corrected)=0.026) whose SRF diverges from that of the
198 sound modality (Fig 5A). For sound, no significant activity prevailed, that is, no relationship of
199 intensity and brain activity was found within the region of interest. Closer inspection of the time-
200 course of the SRF in the heat modality (Fig 5B) indicates that the SRF's maximum slope coincides with
201 the peak of the main effect, that is, the modulation of the main effect by intensity is strongest when
202 the main effect itself is strongest.

203

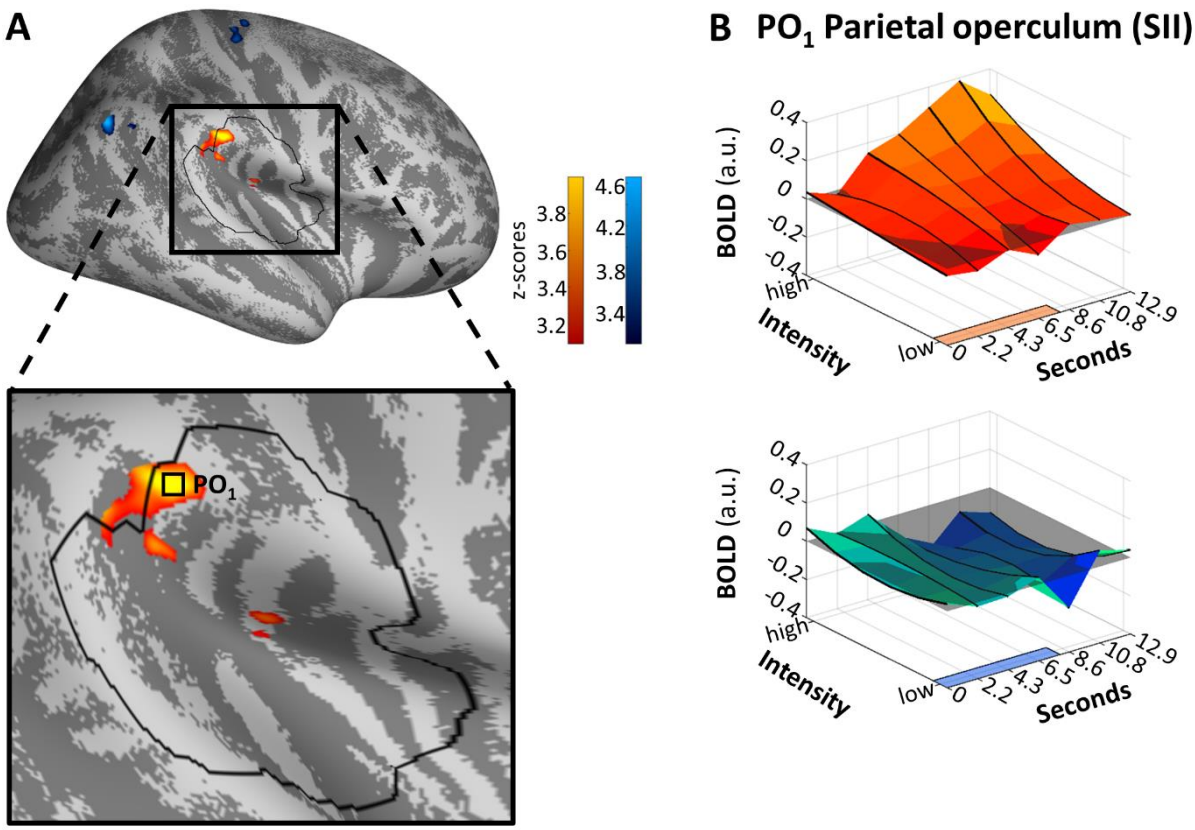

Fig 5. Differential modulation by stimulus intensity for heat (orange) and sound (blue). Significant differences were found in the parietal operculum (PO_1) for heat. **A.** Activations are thresholded at p(uncorrected)<0.001 and overlaid on an average brain surface for display purposes. The black line delineates the region of interest used for correction for multiple comparisons. See S6 Fig for peak positions in brain volume slices. **B.** Poststimulus plots of fMRI activation in vertex PO_1 during heat (orange) and sound (blue). The colored patches at the right axes show the stimulus duration. The lower left (y-)axes show the parametric modulation affecting the main effect (average size of the effect along the lower right (x-)axes): A straight line parallel to the y-axis indicates no change of the BOLD response depending on stimulus intensity, whereas the a sloped main effect along the y-axis indicates parametric modulation. In this area, the main effect of heat is mostly positively modulated by stimulus intensity, that is, higher stimulus intensities induce a higher extent of BOLD. The highest main effect activation occurs around second 10.8 (corresponding to scan 6), coinciding with the steepest slope of parametric modulation by intensity (y-axis).

Again, an unmasked conjunction analysis at a liberal threshold yielded no significant overlap of both modalities, when comparing contrasts with an SRF slope larger than zero for either modality.

Parametric modulation by ratings

Although relevant, physical stimulus intensity might not be directly mapped to neuronal activity, as a sensory signal undergoes multiple levels of processing before it reaches cortical areas. We therefore performed an additional analysis, where we investigated whether areas show BOLD responses that are correlated with subjects' behavioral ratings.

This analysis revealed that activity in the parietal operculum (x=55, y=-37, z=26, Z=5.091, p(corrected)=2e-04; x=58, y=-14, z=18, Z=4.312, p(corrected)=0.008) and the dorsal anterior insula (x=36, y=0, z=14, Z=4.276, p(corrected)=0.009; x=41, y=1, z=14, Z=3.849, p(corrected)=0.047) (Fig 6) showed a positive relationship to perceived intensity. This agrees with and extends results from the previous analysis in which BOLD responses were correlated with stimulus intensity in the parietal operculum. For sound, no significant activity prevailed, that is, no relationship of ratings and brain activity was found.

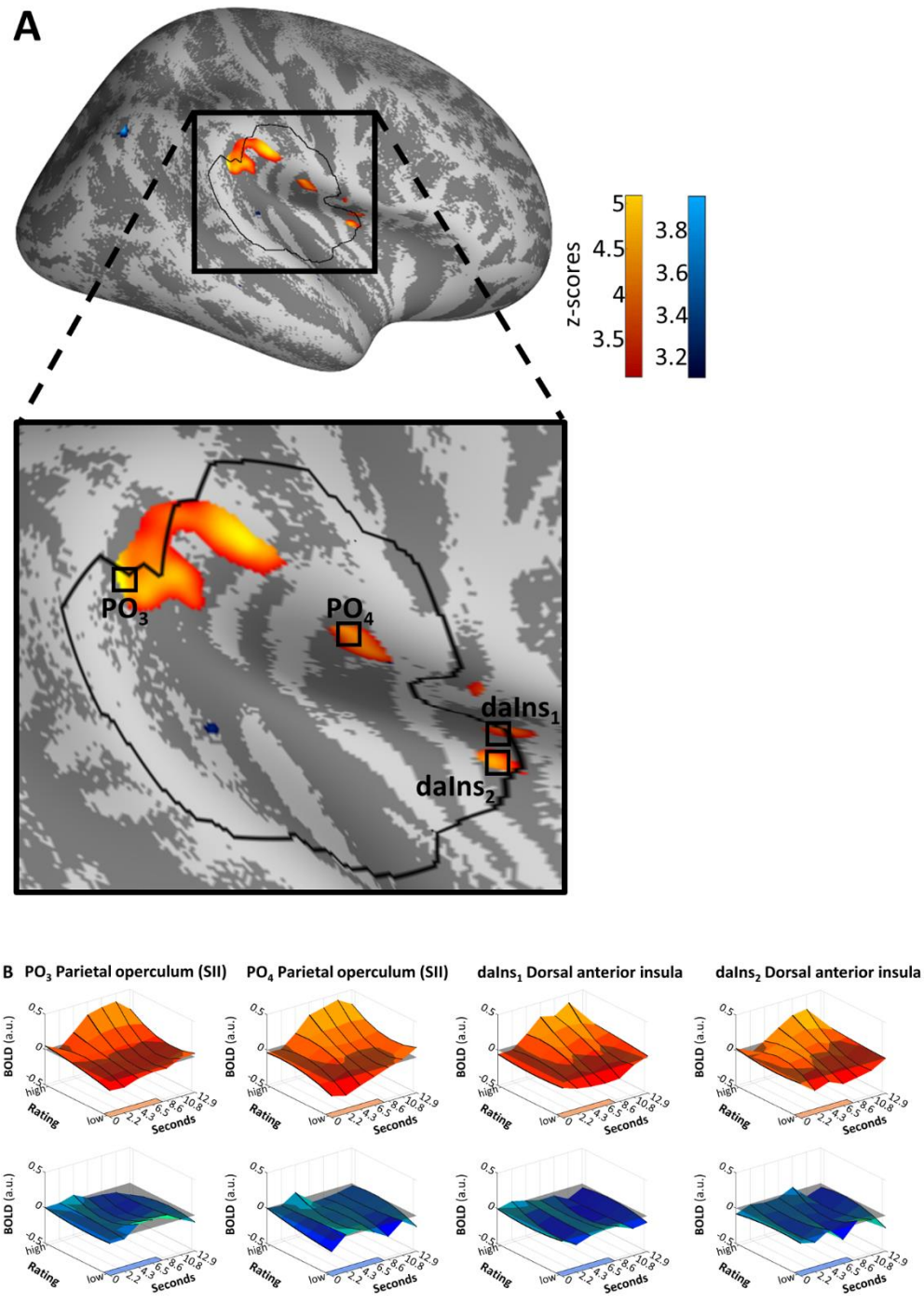

Fig 6. Differential modulation by ratings for heat (orange). Significant differences were found in the parietal operculum (PO_3, PO_4) and dorsal anterior insula ($daIns_1$ and the more ventral $daIns_2$). **A.** Activations are thresholded at p(uncorrected)<0.001 and overlaid on an average brain surface for display purposes. The black line delineates the region of interest used for correction for multiple comparisons. See S7 Fig for peak positions in brain volume slices. **B.** Poststimulus plots of fMRI activation in vertices PO_1, PO_3, $daIns_1$ and $daIns_2$ during

heat (orange) and sound (blue). The colored patches at the right axes show the stimulus duration. The lower left (y-)axes show the parametric modulation by ratings that are affecting the main effect.

As before, in the unmasked conjunction analysis of contrasts where rating correlated with the BOLD responses, no regions with significant overlap were found.

Imaging results distinguishing stimuli perceived below and above thresholds

So far, all analyses pooled over non-painful and painful heat percepts. To further investigate pain-related responses, we separated those stimuli reported as non-painful from those reported as painful (i.e., subthreshold versus suprathreshold), and similarly for unpleasant versus non-unpleasant sounds. We followed an axiomatic approach to identify areas where activity under painful stimulation could neither be explained by an overlap with activity under non-painful heat (as would be the case, e.g., in thermosensitive areas), or by an overlap with activity following unpleasant sound (e.g., in areas processing unspecific characteristics of a stimulus). In particular, we posited that a region can be characterized as preferentially pain-processing if the following conditions hold:

- Axiom 1: The effect of suprathreshold – i.e., painful – stimulation should be larger than that of subthreshold – i.e., heat – stimulation.
- Axiom 2: The effect of suprathreshold heat stimulation should be larger than that of suprathreshold sound stimulation.
- Axiom 3: The relationship of ratings and BOLD – i.e., the slope of the stimulus response function – should be stronger for suprathreshold heat than for subthreshold heat.
- Axiom 4: The relationship of ratings and BOLD should be stronger for suprathreshold heat than for suprathreshold sound.

Each of the axioms was evaluated at a significance threshold of p=0.05, corrected for family-wise error. After joint application of each axiom, analysis revealed activation in the posterior parietal operculum (x=56, y=-37, z=25, Z=3.909, p(corrected)=0.035) (Fig 7), adjacent to the supramarginal gyrus. To broaden the scope, we have performed the same axiomatic analysis on the whole surface with a lower significance threshold of p(uncorrected)=0.001 (S8 Fig). For comparison, results from a conventional 3D analysis are also provided for the whole brain, again with a lower threshold of p(uncorrected)<0.001 (S9 Fig).

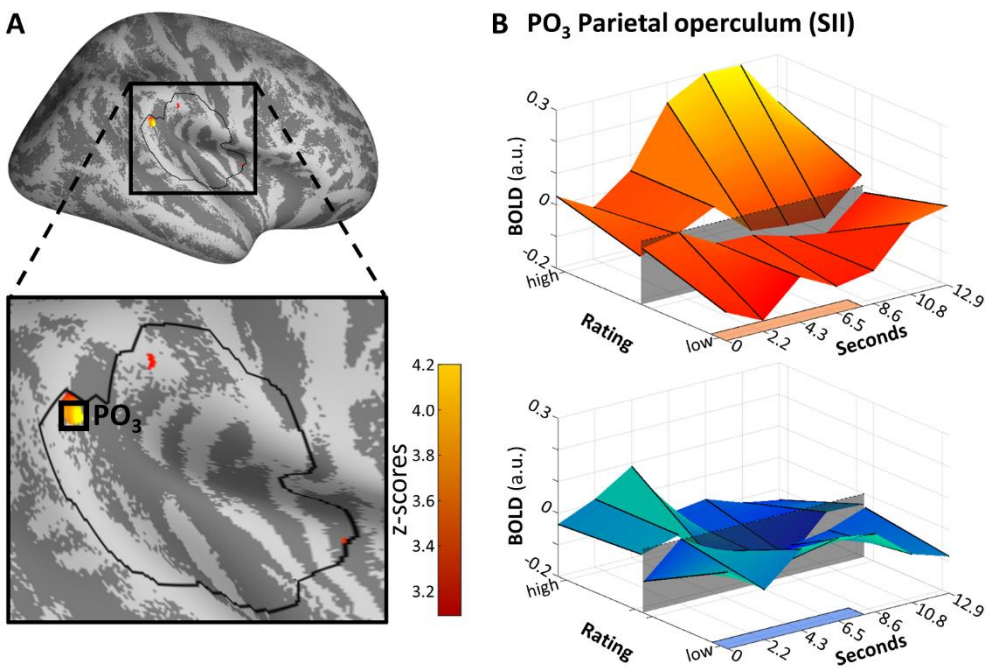

Fig 7. Areas that fulfill the axiomatic requirements of differential activation during pain compared to heat and sound. In detail, these axioms were 1) a larger effect of suprathreshold heat compared to subthreshold heat, 2) a larger effect of suprathreshold heat compared to suprathreshold sound, 3) a stronger relationship of BOLD with pain ratings than with heat ratings, 4) a stronger relationship of BOLD with pain ratings than with unpleasantness ratings. Significant activation was found in the parietal operculum (PO_3). **A.** Activations are thresholded at p(uncorrected)<0.001 and overlaid on an average brain surface for display purposes. The black line delineates the SVC mask. See S10 Fig for peak positions in brain volume slices. **B.** Poststimulus plots of fMRI activation in vertex PO_3 during heat (orange) and sound (blue). The shaded patch in the center signifies the pain

threshold (for heat) and unpleasantness threshold (for sound). The colored patches at the right axes show the stimulus duration.

Discussion

This study aimed to identify regions relevant for heat pain processing, and to determine whether their activation can be explained by salience or other modality-independent characteristics. We used individually calibrated, parametrically graded heat stimuli, and an auditory control condition. Heat and sound stimuli were matched for arousal as indicated by similar skin conductance responses. Furthermore, we employed surface-based analyses to mitigate spatial inaccuracies of 3D smoothing.

Main effects for heat were identified in the parietal operculum and the posterior insula, main effects of acoustic stimuli were observed in the superior temporal gyrus. More importantly, in the parietal operculum, we observed a differential correlation of brain activity with ratings above versus below the heat pain threshold, concurrent with a differential correlation with ratings under painful heat versus unpleasant sound. As we have matched both modalities for salience, these results rule out, within the limitations of this experimental approach, that activity in this area is simply related to stimulus salience, and suggests a more dedicated role in heat pain processing.

Using SCR as an autonomic readout of arousal [24,29–31] allowed us to establish comparable salience of the stimulus material, independent of any behavioral assessments. Although salience can be assessed psychometrically [5] and research exists to establish concurrent validity of salience ratings within individual modalities [32], to our knowledge, such ratings have not been validated cross-modally. It is likely that salience ratings are scaled differently according to some modality-specific perceptual range, that is, a rating of X on a “salience” scale while assessing pain may mean something different from a rating of X while assessing sound, identical scale anchors notwithstanding. To our knowledge, a “ground truth” to compare multiple sensory modalities has never been established in this regard. Our results support the notion of modality-specific scaling, as

we have observed a prevailing difference in behavioral ratings between the two modalities (sound was, on average, rated as more aversive, but had a shallower slope with increasing intensities). This means that a reliance on behavioral ratings alone could compound SCR dissimilarities between comparator modalities.

With six graded stimulus intensities per modality, our design allowed for the assessment of stimulus response functions as opposed to simple mean comparisons between a single intensity and a low-level baseline, or between single sub- and suprathreshold stimuli. Apart from physical intensities, this also allowed us to use a large range of individual ratings as predictors. Using these perceived intensities, we were able to directly investigate competing modes of encoding. For example, a brain area may encode heat intensity, regardless of nociceptive intensity, or it may be inactive below threshold but encode pain intensity above threshold [8,20,21]. In the analysis distinguishing between sub- and suprathreshold stimuli, we see a clear pain intensity-related response in the parietal operculum (Fig 7). While not a main focus of this paper, we do see a shift in SRFs even within small cortical distances: For example, an area rostral (x=55, y=-26, z=26) to the posterior parietal operculum cluster identified in the axiomatic analyses (x=56, y=-37, z=25) fails to register differences in the parametric modulation by sub- versus suprathreshold heat (Fig 8).

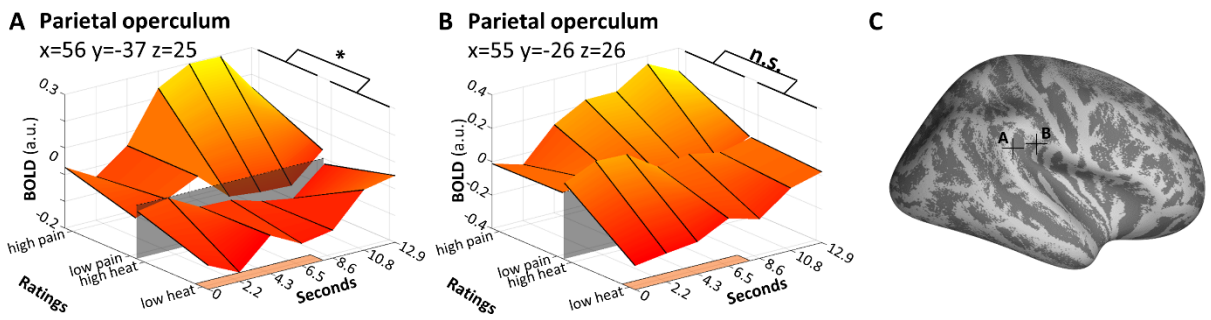

Fig 8. Distinction of areas with stimulus response functions corresponding to the axioms, or not (heat modality only). **A.** The slopes of subthreshold (heat) versus suprathreshold (pain) activation as described in Fig 7, corresponding to parietal operculum cluster 3 (PO_3). Heat slopes are shallower than pain slopes. **B.** Slopes of heat and pain activation in an opercular vertex slightly anterior to A (corresponding to PO_2), as determined per

329 conjunction of heat and pain parametric modulation. Slopes are more aligned, preventing the contrasted
330 activation (pain>heat) of reaching significance. Note that this is not a formal comparison to A. **C.** Location of the
331 vertices described in A and B. B is in an adjacent area about 1 cm surface distance rostral from A.

332

333 Areas in the insula and surrounding cortical areas are characterized by extreme cortical folding. We
334 therefore implemented a subject-specific surface-based fMRI analysis. This prevents contamination
335 of gray matter voxels by signal from white matter and cerebrospinal fluid. Furthermore, surface-
336 based analyses circumvent potential issues arising from three-dimensional smoothing which
337 accidentally mixes signals from structures adjacent in three-dimensional space which are actually
338 distant from each other. For example, the parietal operculum is directly adjacent to the superior
339 temporal gyrus in three-dimensional space, but their neurons are separated by the entire insular
340 fold. Smoothing with a three-dimensional kernel therefore includes activity across the lateral sulcus
341 (alongside noise from white matter and corticospinal fluid), thereby increasing error terms and
342 decreasing sensitivity of the respective comparisons. Importantly, in this case, three-dimensional
343 smoothing could also generate erroneous overlaps between conditions. Surface-based analyses have
344 been found to increase sensitivity and reduce deviations when normalizing from native to standard
345 space [33].

346 In contrast to previous multimodal studies, we explicitly chose modalities where the aversiveness
347 would be generated by virtue of physical intensity. This is naturally the case with painful stimulation,
348 but several studies did not use aversive stimulation in non-painful control modalities (for example
349 [11], who used low-intensity tactile stimulation). Consequently, the acoustic modality was chosen
350 because stimuli can be generated in close analogy to heat, by altering the physical intensity of the
351 stimuli.

352 For our analyses of neuronal activity, we have focused on the posterior insula and adjacent areas.
353 The insula is of particular interest, because its involvement in pain has been well-documented

354 [4,11,34]. Furthermore, it has been hypothesized to perform polymodal magnitude estimation [8,35],
355 and is also involved in threat learning [36] and salience processes [37,38]. Unambiguous data
356 concerning the involvement of the insular cortex in pain processing also comes from direct cortical
357 stimulation studies [39–41]. Consequently, it is a prime candidate to assess overlaps and differences
358 in activation patterns.

359 With its reliable activation following painful stimulation and within the constraints inherent in our
360 experimental approach, we can corroborate the role of the parietal operculum as an important area
361 of heat pain processing, and importantly, one whose activity cannot be explained by unspecific
362 characteristics of sensory stimulation, like stimulus salience. The area not only shows increased
363 activation when comparing pain and other modalities (heat, sound), but also exhibits a monotonic
364 increase with perceived pain. The peak of the BOLD response following pain clearly coincides with
365 the largest modulation by behavioral ratings of pain, roughly 8 seconds after stimulus onset (Fig 7B).
366 Importantly, this area has close functional connections with the posterior insula [42], another area of
367 interest [11,25]. Contextualization of this finding with previous studies comparing at least two
368 stimulus modalities [5,8,13,43] is difficult, because their modality-matching was performed on
369 ratings of salience and/or intensity (not SCR), or used only a single stimulus intensity per modality
370 (i.e., a comparison of main effects). With these caveats in mind, one study found activation at similar
371 coordinates for painful stimulation (x=56, y=-36, z=28) and the visual control condition (x=62, y=-36,
372 z=20), but no preferential activation following pain [8]. Mouraux and colleagues [5] likewise reported
373 no preferential S2 activation following painful stimulation, but an increased activation during
374 (noxious and non-noxious) somatosensory stimulation compared to acoustic and visual. Another
375 study reanalyzed two studies (including [5]) and identifies a proximate cluster (x≈53, y≈-27, z=27) as
376 "pain-preferring" in the sense that activation was consistently higher compared to all three control
377 modalities [43]. The last study used a tactile control condition and did not report preferential
378 activation of the cluster following painful stimulation [13].

Previous studies have shown a considerable overlap of brain activity following stimulation in different sensory modalities [5,13,14]. The extent of any overlap in functional neuroimaging is strongly dependent on the statistical threshold employed, and it is possible that diverging results stem from different thresholding or conjunction methods. However, for reasons of comparability we wish to mention that our data shows no such overlap of activation across modalities, even at a low threshold. While other differences in imaging analysis exist between the studies (for example, we have performed analysis on the brain surface), the lack of overlap might rather be related to the differences in stimulus parameters: Previous multisensory studies have used rapid onset stimuli of very short duration [5,13,14], whereas ours were considerably longer (8 seconds plateau, circa 9.5 seconds with upward/downward slopes). It is possible that with increasing brevity and suddenness of the stimuli, the extent of unspecific orientation responses and other attention related processes is disproportionally larger, and therefore a larger overlap of neuronal activation can be observed [44]. If true, this overlap would naturally be determined, to a large extent, by unspecific and not pain-related activations such as salience.

Brain responses evoked by stimuli in different sensory modalities might follow different time courses; systematic differences may, for example, arise from different conduction speeds of fibers relaying auditory (mostly very fast Aα fibers), thermoceptive (mostly slow C fibers) and nociceptive input (Aδ and C fibers), compounded by the fact that thermal stimulation (in this setup) occurs at a distal site compared to auditory stimulation. Therefore, in analogy to [5], we opted for analyzing the time-course of all imaging data by using finite impulse responses as basis functions. This largely avoids the constraints and biases implicit in comparing mean activations obtained by pre-defined hemodynamic response functions.

Some limitations apply to the present research. Importantly, due to the salience-matching approach based on skin conductance, a substantial number of study participants were not eligible for inclusion, because they either did not show a stimulus-intensity related SCR, or showed responses skewed towards the heat modality. This procedure could induce a sampling bias, for example by selecting

subjects with stronger SCR reactivity, which could implicate different salience network connectivity [45]. However, we found no difference in calibrated intensities in pain or sound or their variance when comparing included versus excluded subjects (all $p>0.5$; see S3 Tab), making a sampling bias unlikely.

As additional limitation, the study used stimuli of mild to moderate aversiveness (calibrated to a maximum of 50 if rescaled to a conventional, 0-100 suprathreshold visual analogue scale). This aspect, too, could be amended to cover a broader range, albeit increasing the risk of carry-over effects such as sensitization, particularly with longer stimulus duration. Furthermore, the use of only a single trial-based, post-stimulus rating of stimulus intensity could be criticized. In fact, one common recommendation for pain measurement is to distinguish multiple pain dimensions [1], most frequently intensity and unpleasantness [46], although these aspects tend to be highly correlated in non-interventional designs [47,48]. Given the SCR-based approach to equalize salience and to include more stimulus repetitions, we opted against multiple VAS for protocol reasons, namely ease of measurement and to avoid confusion.

While we have identified areas preferentially active in painful heat as compared to unpleasant sound, we cannot claim that these areas are specific for pain. In fact, it is important to note that specificity cannot be ascertained with a limited number of control conditions [19,49]. We concur that the notion of specificity is more academic in nature than might benefit the field [3]. The preferences of certain areas to process various inputs – whether visual, acoustic, nociceptive – is best construed as a matter of degree, that is, a question of specialization rather than specificity, as has been suggested for functions unrelated to pain [50]. Nevertheless, the rigorous axiomatic approach allows for a strong hypothesis ascribing the parietal operculum a dedicated role in pain processing.

428 ## Materials and Methods

429 The protocol was approved by the local Ethics Committee (Ethikkommission der Ärztekammer
430 Hamburg, vote PV4745) and conformed to the standards laid out by the World Medical Association in
431 the Declaration of Helsinki. Participants gave written informed consent prior to participation.

432

433 *Exclusion criteria*

434 A list of exclusion criteria is provided in Table 1.

435

436 **Table 1.** Exclusion criteria.

- Age younger than 18, older than 40
- Sufficient visual acuity, correction with contact lenses only
- Conditions disqualifying for MR-scanners (e.g. claustrophobia, wearing a pacemaker)
- Ongoing participation in pharmacological studies, or regular medication intake (e.g. analgesics)
- Analgesics use 24h prior to the experiment
- Pregnancy or breastfeeding
- Chronic pain condition
- Manifest depression (as per Beck Depression Inventory II, BDI-II, cutoff 14 as per [51])
- Somatic symptom disorder (as per Patient Health Questionnaire, PHQ15, cutoff 10 as per [52])
- Other neurological, psychiatric or dermatological conditions
- Inner ear conditions
- Head circumference >60 cm (for second cohort, due to device constraints)

437

438 *Psychophysiological recordings*

439 Electrodermal activity was measured with MRI-compatible electrodes on the thenar and hypothenar
440 of the left hand. Electrodes were connected to Lead108 carbon leads (BIOPAC Systems, Goleta, CA,
441 USA). The signal was amplified with an MP150 analog amplifier (also BIOPAC Systems). It was
442 sampled at 1000 Hz using a CED 1401 analog-digital converter (Cambridge Electronic Design,
443 Cambridge, UK) and downsampled to 100 Hz for analysis.

444 Analysis was performed using the Ledalab toolbox for MATLAB [53]. Single subject data were
445 screened for artifacts which were removed if possible by using built-in artifact correction algorithms.
446 Using a deconvolution procedure, we computed phasic skin conductance (SCR). SCR occurring after
447 stimulus onset and within stimulus duration was used for measuring autonomic arousal. Response
448 windows were defined by visual inspection, per modality: between 2.0 s and 4.5 s for heat, and
449 between 1.5 s and 4.0 s for sound. Results were log- and z-transformed to reduce the impact of intra-
450 and interindividual outliers [24]. Subsequently, SCR was averaged within subjects for two modalities
451 (heat/sound) and six stimulus intensities each, yielding twelve values per person.

452 SCR was used because it is an objective measure of general sympathetic activity, and therefore a
453 measure of arousal, stimulus salience and several associated psychological processes [24,29–31]. It is
454 is routinely used in assessing painful [23,54,55] as well as acoustic stimulation [56].

455

456 *fMRI acquisition and preprocessing*

457 Functional and anatomical imaging was performed using a TRIO 3T MR Scanner (Siemens, Erlangen,
458 Germany) with a 12-channel head coil. An fMRI sequence of 36 transversal slices of 2 mm thickness
459 was acquired using T2*-weighted gradient echo-planar imaging (EPI; 2150 ms TR, 25 ms TE, 80° flip
460 angle, 2x2x2 mm voxel size, 1 mm gap, 216x216x107 mm field of view, acceleration factor of 2 with
461 generalized autocalibrating partially parallel acquisitions reconstruction, GRAPPA). Coverage did not

include the apical parts of the frontal/parietal lobes. Additionally, a T1-weighted MPRAGE anatomical image was obtained for the entire head (voxel size 1x1x1 mm, 240 slices).

For each subject, fMRI volumes were realigned to the mean image in a two-pass procedure, and co-registered to the anatomical image using affine transformations. Anatomical images were segmented into tissue types, and individual brain surfaces generated, using the CAT12 toolbox for SPM (Christian Gaser & Robert Dahnke, http://www.neuro.uni-jena.de/cat/).

Analysis of imaging data

Subject-level analyses were performed on the 3D (volume) data in native space without smoothing, using an implicit mask at 0.6 to facilitate subsequent (surface) processing. We computed general linear models to identify brain structures involved in the processing of each stimulus modality, as well as the encoding of intensities within those modalities. All analyses were performed with seventh order FIR basis functions, of which bins 2 to 6 are considered when comparing conditions. This amounts to seconds 2.2 through 10.8 post stimulus onset. Realignment (motion) parameters as well as regressors obtained from ventricular motion were included as nuisance variables, to mitigate motion-related artifacts.

We first set up a model including one regressor for stimulus main effects in each modality. Another two regressors – one linear, one quadratic – encoding stimulus intensities 1 through 6 were added per modality, as parametric modulators. The second model likewise included main effects, and behavioral ratings as linear and quadratic parametric modulators. Finally, the third model further distinguished the two modalities in stimuli perceived as below and above the respective thresholds (pain for heat stimuli, unpleasantness for sound stimuli), yielding four main effect regressors (subthreshold heat, suprathreshold heat – i.e., pain –, subthreshold sound, suprathreshold sound). Behavioral ratings were again included as linear parametric modulators; quadratic modulation was not considered to preclude overfitting.

487 Results from subject-level analyses were mapped to brain surfaces obtained via the CAT12
488 segmentation procedure. The mapped subject-level results were then resampled to correspond to
489 surface cortical templates, and smoothed with a 6 mm full width-half maximum 2D kernel. Group-
490 level analyses were performed including the mapped contrasts, which are described in the Results
491 section.

492 Masking was used to distinguish either modality, as the ANOVAs employed are unsigned and in
493 principle detect differences in activation regardless of direction. Therefore, we obtained signed (that
494 is, unconstrained by p values) masks from calculating a conjunction from significant voxels of a) a t-
495 test contrasting the average main effects of either modality (i.e., where activation following heat was
496 larger than that following sound, and vice versa), and b) a t-test contrasting either modality to low-
497 level baseline (i.e., where activation following heat – or sound, respectively – was larger than zero.
498 This yielded a single mask for both modalities, which was applied to all analyses (unless otherwise
499 noted) (S1B Fig).

500 For the purpose of this study, we focused on the hemisphere contralateral to the stimulation, in our
501 case the right hemisphere. In general, the larger part of activity following pain is contralateral to the
502 stimulation site, but is known to be bilateral in several key areas such as the secondary
503 somatosensory cortex and the insula [22].

504 Furthermore, we focused on the insula and directly adjacent areas for small volume correction of
505 significance level. In particular, we included the granular insular cortex (Ig1, Ig2) as well as the
506 parietal operculum (OP1, OP2) and primary auditory cortex (Te1.1), using the SPM Anatomy Toolbox
507 (version 2.2b [57]). This mask was mapped to a template brain surface, then smoothed with a 4 mm
508 2D kernel to close gaps. The resulting binary mask (S1A Fig) was roughly centered around previously
509 reported coordinates (x=[-]34, y=-20, z=18) involving areas putatively dedicated to pain processing
510 [11]. It was used for small volume correction of second level analyses, where results were considered
511 after correction for family-wise error rate of $p<0.05$.

Psychometry

Owing to the study's aim to compare two stimulus modalities (heat and sound), they had to be presented and rated in an analogous fashion. Therefore, while retaining the intuitive descriptor "painfulness" for rating noxious heat (as composite measure of intensity and unpleasantness), we settled on "unpleasantness" as descriptor for sounds. This also seemed warranted considering the high correlation of intensity and unpleasantness measures in heat pain [48], while unpleasantness is one of the definitional criteria of pain [2].

Furthermore, since we wanted to use graded stimuli both below and above the respective thresholds (pain threshold for heat, unpleasantness threshold for sound), we deviated from the more common simple visual analogue scales (VAS) and devised two partitioned 0 to 100 VAS for both modalities (Fig 1A).

For heat, it captured both painful and non-painful sensations. Subjects were instructed to indicate heat intensity in absence of pain in the 0 through 49 range, and heat pain intensity in the 50 through 100 range. Hence, anchors were displayed for "no sensation" (0), "minimal pain" (50), and "unbearable pain" (100). Pain was operationalized as the presence of sensations other than pure heat intensity, such as stinging or burning, as per the guidelines of the German Research Network on Neuropathic Pain [58].

Likewise, for sound, both unpleasant and non-unpleasant sensations were captured by the VAS. Subjects were instructed to indicate loudness in absence of unpleasantness in the 0 through 49 range, and loudness unpleasantness in the 50 through 100 range. Anchors were displayed for "inaudible" (0), "minimally unpleasant" (50), and "extremely unpleasant" (100). Unpleasantness was operationalized as a bothersome quality of the sound emerging at a certain loudness.

536 *Heat stimuli and calibration*

537 Heat stimuli were delivered using a CHEPS thermode (Medoc, Ramat-Yishai, Israel). Stimulation sites
538 were located on the radial surface of the forearm. Three separate sites were used for calibration and
539 either experimental session, to avoid changes in heat/pain perception due to repeated stimulation.
540 Around the middle of the forearm (half distance between crook of the arm and distal wrist crease;
541 see Fig 1B), three stimulation sites were marked prior to the experimental sessions. For calibration, a
542 medial site on the distal part of the forearm was used; for experimental sessions 1 and 2, two
543 adjacent proximal sites were used, in counterbalanced order. During both calibration procedure and
544 experimental sessions, baseline temperature was set to 35°C, and rise and fall rate were set to 15°C
545 per second. The duration of heat stimuli was set to eight seconds at target temperature (plateau),
546 except for preexposure stimuli whose plateau duration was zero (and thus only consisted of
547 temperature up- and downramping).

548 A two-step stimulus calibration was performed for each subject, to determine three temperatures
549 below the individual pain threshold, and three above. Calibration was performed with the MR-
550 scanner running the same sequence as during the actual experimental sessions, to mimic ambient
551 conditions [59]. fMRI data from calibration was later discarded.

552 In a first calibration step, the pain threshold was determined. Subjects were preexposed to four brief
553 heat stimuli. Preexposure started at 42°C and each consecutive stimulus was increased by 0.5°C, up
554 to 43.5°C. If a subject indicated the last stimulus as painful, starting temperature for the following
555 procedure was set to 43°C, else to 44°C. We then used a probabilistic tracking procedure for
556 threshold determination, assuming a normal distribution of pain perception around the actual
557 threshold [60]. Eight full-length stimuli were presented and received a binary rating (painful or not
558 painful). Depending on the rating of the previous stimulus, each consecutive stimulus was set to a
559 higher or lower temperature according to the probability informed by previous pivot points. The final
560 temperature was defined as threshold intensity.

561 In a second calibration step, eight stimuli unevenly spaced around threshold intensity (from -2°C to
562 +1.6°C, with smaller intervals towards ±0°C) were rated on the partitioned VAS described above.
563 After the procedure, linear regression was used to calculate target temperatures H1 through H6, to
564 obtain subthreshold VAS ratings of 25, 35 and 45 (H1–H3), and suprathreshold VAS ratings of 55, 65
565 and 75 (H4–H6).

566 These six intensities were used throughout the experimental sessions.

567

568 *Sound stimuli and calibration*

569 Sound stimuli were delivered using MR-compatible headphones (NordicNeuroLabs, Bergen, Norway).
570 A pure sound (frequency 1000 Hz, sampling rate 22050 Hz) was generated using MATLAB. A log
571 function was used to translate increases in (physical) amplitude to smooth gradual increases in
572 (psychoacoustic) loudness, to mimic the heat stimuli's temperature ramps. Like the heat stimuli,
573 sound stimuli were presented for eight seconds at target loudness (plateau), and the scanner was
574 running a dummy EPI sequence throughout to mimic actual conditions [61].

575 A two-step stimulus calibration was performed for each subject, to determine three sounds below
576 the individual unpleasantness threshold, and three above. The general procedure was analogous to
577 the one used for heat.

578 In a first calibration step, the individual loudness unpleasantness threshold (in percent of maximum
579 amplitude of ~100 dB, allowing for safe exposure even at maximum intensities [62]) was determined
580 by an ascending methods of limits-procedure. Six sounds of gradually increasing loudness were
581 played. The calibration sounds differed in the steepness of the loudness ramps, taking between 9 and
582 15 seconds to reach peak amplitude. Subjects were asked to indicate the point where the loudness
583 became unpleasant. The mean of the last four of the six stimuli was defined as threshold loudness.

584 In a second calibration step, 16 stimuli unevenly spaced around threshold loudness were presented
585 (from -15% to +15%, smaller intervals towards ±0%), with stimulus characteristics set to mimic those
586 of heat stimuli (roughly 0.75 s ramps up and down, plus 8 s plateau loudness). As with heat ratings,
587 linear regression was used to calculate target amplitudes S1 through S6, namely to obtain
588 subthreshold VAS ratings of 25, 35 and 45 (S1–S3), and suprathreshold VAS ratings of 55, 65 and 75
589 (S4–S6). For the second cohort, VAS targets were informed by the corresponding mean SCR
590 amplitude of the first cohort (see "Differences between first and second cohort").

591 Finally, ramping characteristics of sound stimuli (the seconds it took to plateau) were set to
592 correspond to those of the respective intensity's heat stimuli, such that corresponding intensities of
593 both modalities had an identical overall length (ramps plus plateau).

594

595 *Stimulus presentation during experimental sessions*

596 After calibration, the thermode stimulation site was changed, and the first experimental session
597 commenced. Heat and sound stimuli were presented in alternation, so that trials of the same
598 modality were spaced with an intertrial interval of approximately 30 seconds. Each trial followed the
599 same basic structure (Fig 1C).

600 Within each modality, the six intensities were pseudorandomized in microblocks. Randomization was
601 performed such that each sequence of six stimuli contained one instance of each intensity. It was
602 further constrained such that the very first stimulus was never chosen from the highest two
603 intensities, and two consecutive intensities were never more than 3 intensity steps different (e.g.,
604 the intensity following heat intensity 1 could not exceed heat intensity 4).

605 After changing thermode stimulation site again, session 2 commenced with identical protocol (albeit
606 different randomization).

607 Visual cues and VAS rating scales were displayed in the scanner using back-projection via a 45° mirror
608 placed atop the head coil.

609

610 *Selection of subsample for analysis with comparable SCR between modalities*

611 In total we assessed two cohorts of 32 subjects and 26 subjects. To obtain an "SCR-equalized"
612 subsample from all subjects (N=58 with 2 sessions, that is a total of 116 experimental sessions), in a
613 first step, we excluded all sessions where the correlation between ratings (that is, perceived stimulus
614 intensity/unpleasantness) and SCR was lower than or equal to zero, so that only subjects with a
615 positive correlation in both modalities were eligible for the next step.

616 In a second step, we used Bayes factors [63,64] to determine the flipping point where modality
617 became obsolete as explanatory variable. Bayes factors express the ratio of the marginal likelihood of
618 the data under the compared models; since they consider the number of free parameters, they allow
619 for the selection of the "better" model (best fit to the data and most parsimonious). For every
620 session, we obtained the mean SCR (log-transformed and normalized values) for both modalities;
621 sessions with the largest predominance of heat-SCR were then consecutively removed. After each
622 removal, we obtained the Bayes factors for the remaining sample, comparing the model with
623 intensity only as predictor to that with modality added as predictor. Once the Bayes factor dropped
624 below 1 (meaning that the addition of modality as predictor did not serve to improve the model), we
625 stopped the pruning procedure. This relatively permissive criterion for session inclusion was chosen
626 in order to preserve as many sessions as possible.

627 This procedure yielded a sample where modality did not contribute to explaining the SCR data, with
628 26 unique subjects contributing 33 sessions. From the first cohort, 15 subjects contributed 19
629 sessions, from the second cohort, 11 subjects contributed 13 sessions to the SCR-equalized analysis.

630

Differences between first and second cohort

Since we had determined that not every person's skin conductance responded to both modalities to a comparable extent, we set out to select a subsample of persons who had comparable SCR. To reach a sufficient number of such "responders", we had to perform an additional data collection.

Because of logistical reasons (scanner upgrade in January 2018), some parameters of fMRI acquisition had to be modified for the new PRISMA 3T MR Scanner (Siemens, Erlangen, Germany). Instead of a 12-channel head coil, we had to employ a 20-channel head coil. Delivery of the auditory stimulus was performed with a CONFON headphone (Cambridge Research Systems Ltd, Rochester, United Kingdom). These measures necessitated the exclusion of subjects with head circumference above 60cm.

Furthermore, to facilitate increased SCR responding to sound, we increased the amplitude of the sound stimuli. Using calibration data from the first data collection and linear extrapolation, we calculated sound VAS targets required to induce SCRs of an amplitude comparable to those of heat VAS targets of the same intended intensity 1 through 6. We determined that corresponding to our heat VAS targets of 25, 35, 45, 55, 65, 75 (see "Heat stimuli and calibration"), we would need to apply sound amplitudes inducing sound VAS targets of 48, 59, 70, 82, 93, 105. Furthermore, during subject instruction, we emphasized the fact that the amplitude of sound stimuli was not within pathological range. This was done to prevent overly cautious subject behavior, following anecdotal evidence from the first cohort that sound stimuli were associated with higher safety concerns than heat stimuli.

Statistical analyses

All analyses were performed using MATLAB (version R2017b) and SPM12 (version 6906).

Significance level was set to $p=0.05$ for psychophysiological and behavioral data, whereas imaging results were corrected using family-wise error rate adjustment at $p<0.05$. For visualization,

activations are thresholded at p(uncorrected)<0.001 and overlaid on an average brain surface. All coordinates are reported in Montreal Neurological Institute (MNI) space.

Skin conductance data and behavioral ratings were analyzed using linear mixed models with random intercepts [65], with centering of predictors following recommendations [66].

Group-level analyses of imaging data were performed as within-subjects ANOVA (cf. “Analysis of imaging data” above, and the respective Results sections).

Acknowledgements

This work was supported by European Research Council Advanced Grant ERC-2010-AdG_20100407 and Deutsche Forschungsgemeinschaft Grant SFB 936 Project A06. Björn Horing was supported by the Alexander von Humboldt-Foundation (Feodor Lynen Return Fellowship). We thank Jürgen Finsterbusch, Katrin Bergholz, Waldemar Schwarz and Kathrin Wendt for technical assistance during MR data collection, and Lara Austermann, Tim Dretzler, Katharina Ebel and Matthias Kerkemeyer for their assistance with data collection, and finally Christian Gaser for helpful comments concerning the CAT12 toolbox.

Conflicts of interest

The authors declare no conflict of interest.

Corresponding author

Correspondence should be addressed to Dr. Björn Horing, Department of Systems Neuroscience, University Medical Center Hamburg-Eppendorf, Martinistrasse 52, 20246 Hamburg, Germany. b.horing@uke.de

678 **References**

679 1. Moayedi M, Davis KD. Theories of pain: from specificity to gate control. J Neurophysiol.
680 2013;109(1):5–12. doi: 10.1152/jn.00457.2012

681 2. International Association for the Study of Pain (IASP). Pain terms: a list with definitions and
682 notes on usage. Recommended by the IASP Subcommittee on Taxonomy. Pain. 1979;6(3):249.

683 3. Tracey I, Mantyh PW. The cerebral signature for pain perception and its modulation. Neuron.
684 2007;55(3):377–91. doi: 10.1016/j.neuron.2007.07.012

685 4. Garcia-Larrea L, Peyron R. Pain matrices and neuropathic pain matrices: A review. Pain.
686 2013;154:S29–43. doi: 10.1016/j.pain.2013.09.001

687 5. Mouraux A, Diukova A, Lee MC, Wise RG, Iannetti GD. A multisensory investigation of the
688 functional significance of the "pain matrix." Neuroimage. 2011;54(3):2237–49. doi:
689 10.1016/j.neuroimage.2010.09.084

690 6. Legrain V, Iannetti GD, Plaghki L, Mouraux A. The pain matrix reloaded: A salience detection
691 system for the body. Prog Neurobiol. 2011;93(1):111–24. doi:
692 10.1016/j.pneurobio.2010.10.005

693 7. Ploghaus A, Tracey I, Gati JS, Clare S, Menon RS, Matthews PM, et al. Dissociating pain from its
694 anticipation in the human brain. Science. 1999;284(5422):1979–81.

695 8. Baliki MN, Geha PY, Apkarian A V. Parsing pain perception between nociceptive
696 representation and magnitude estimation. J Neurophysiol. 2009;101(2):875–87. doi:
697 10.1152/jn.91100.2008

698 9. Davis KD, Bushnell MC, Iannetti GD, St Lawrence K, Coghill R. Evidence against pain specificity
699 in the dorsal posterior insula. F1000Research. 2015;4(2):362. doi:
700 10.12688/f1000research.6833.1

701 10. Salomons T V., Iannetti GD, Liang M, Wood JN. The “pain matrix” in pain-free individuals.
702 JAMA Neurol. 2016;73(6):4–5. doi: 10.1001/jamaneurol.2016.0653

703 11. Segerdahl AR, Mezue M, Okell TW, Farrar JT, Tracey I. The dorsal posterior insula subserves a
704 fundamental role in human pain. Nat Neurosci. 2015;18(4):499–500. doi: 10.1038/nn.3969

705 12. Büchel C, Geuter S, Sprenger C. Comparing Painful Stimulation vs Rest in Studies of Pain.
706 JAMA Neurol. 2016;73(10):1258. doi: 10.1001/jamaneurol.2016.2989

707 13. Su Q, Qin W, Yang QQ, Yu CS, Qian TY, Mouraux A, et al. Brain regions preferentially
708 responding to transient and iso-intense painful or tactile stimuli. Neuroimage. 2019;192:52–
709 65. doi: 10.1016/j.neuroimage.2019.01.039

710 14. Liberati G, Klöcker A, Safronova MM, Ferrão Santos S, Ribeiro Vaz J-G, Raftopoulos C, et al.
711 Nociceptive Local Field Potentials Recorded from the Human Insula Are Not Specific for
712 Nociception. PLOS Biol. 2016;14(1):e1002345. doi: 10.1371/journal.pbio.1002345

713 15. Liberati G, Klöcker A, Algoet M, Mulders D, Maia Safronova M, Ferrao Santos S, et al. Gamma-
714 Band Oscillations Preferential for Nociception can be Recorded in the Human Insula. Cereb
715 Cortex. 2018;28(10):3650–64. doi: 10.1093/cercor/bhx237

716 16. Wager TD, Atlas LY, Lindquist MA, Roy M, Woo C-W, Kross E. An fMRI-based neurologic
717 signature of physical pain. N Engl J Med. 2013;368(15):1388–97. doi:
718 10.1056/NEJMoa1204471

719 17. Kragel PA, Kano M, Van Oudenhove L, Ly HG, Dupont P, Rubio A, et al. Generalizable
720 representations of pain, cognitive control, and negative emotion in medial frontal cortex. Nat
721 Neurosci. 2018;21(2):283–9. doi: 10.1038/s41593-017-0051-7

722 18. Hu L, Iannetti GD. Painful Issues in Pain Prediction. Trends Neurosci. 2016;39(4):212–20. doi:
723 10.1016/J.TINS.2016.01.004

724 19. Mouraux A, Iannetti GD. The search for pain biomarkers in the human brain. Brain.

725 2018;141(12):3290–307. doi: 10.1093/brain/awy281

726 20. Bornhövd K, Quante M, Glauche V, Bromm B, Weiller C, Büchel C. Painful stimuli evoke
727 different stimulus-response functions in the amygdala, prefrontal, insula and somatosensory
728 cortex: a single-trial fMRI study. Brain. 2002;125(Pt 6):1326–36.

729 21. Loggia ML, Edwards RR, Kim J, Vangel MG, Wasan AD, Gollub RL, et al. Disentangling linear
730 and nonlinear brain responses to evoked deep tissue pain. Pain. 2012;153(10):2140–51. doi:
731 10.1016/j.pain.2012.07.014

732 22. Coghill RC, Sang CN, Maisog JM, Iadarola MJ. Pain Intensity Processing Within the Human
733 Brain: A Bilateral, Distributed Mechanism. J Neurophysiol. 1999;82(4):1934–43. doi:
734 10.1152/jn.1999.82.4.1934

735 23. Tiemann L, Hohn VD, Ta Dinh S, May ES, Nickel MM, Gross J, et al. Distinct patterns of brain
736 activity mediate perceptual and motor and autonomic responses to noxious stimuli. Nat
737 Commun. 2018;9(1):4487. doi: 10.1038/s41467-018-06875-x

738 24. Boucsein W. Electrodermal activity. 2nd ed. New York: Springer; 2012.

739 25. Bastuji H, Frot M, Perchet C, Hagiwara K, Garcia-Larrea L. Convergence of sensory and limbic
740 noxious input into the anterior insula and the emergence of pain from nociception. Sci Rep.
741 2018;8(1):13360. doi: 10.1038/s41598-018-31781-z

742 26. Bastuji H, Frot M, Perchet C, Magnin M, Garcia-Larrea L. Pain networks from the inside:
743 Spatiotemporal analysis of brain responses leading from nociception to conscious perception.
744 Hum Brain Mapp. 2016;37(12):4301–15. doi: 10.1002/hbm.23310

745 27. Pomares FB, Faillenot I, Barral FG, Peyron R. The “where” and the “when” of the BOLD
746 response to pain in the insular cortex. Discussion on amplitudes and latencies. Neuroimage.
747 2013;64:466–75. doi: 10.1016/j.neuroimage.2012.09.038

748 28. Roy M, Shohamy D, Daw N, Jepma M, Wimmer GE, Wager TD. Representation of aversive

749 prediction errors in the human periaqueductal gray. Nat Neurosci. 2014;17(11):1607–12. doi:
750 10.1038/nn.3832

751 29. D'Hondt F, Lassonde M, Collignon O, Dubarry A-S, Robert M, Rigoulot S, et al. Early brain-body
752 impact of emotional arousal. Front Hum Neurosci. 2010;4:33. doi:
753 10.3389/fnhum.2010.00033

754 30. Bradley MM, Codispoti M, Cuthbert BN, Lang PJ. Emotion and motivation I: Defensive and
755 appetitive reactions in picture processing. Emotion. 2001;1(3):276–98. doi: 10.1037/1528-
756 3542.1.3.276

757 31. Critchley HD. Review: Electrodermal Responses: What Happens in the Brain. Neurosci.
758 2002;8(2):132–42. doi: 10.1177/107385840200800209

759 32. Kayser C, Petkov CI, Lippert M, Logothetis NK. Mechanisms for Allocating Auditory Attention:
760 An Auditory Saliency Map. Curr Biol. 2005;15(21):1943–7. doi: 10.1016/j.cub.2005.09.040

761 33. Hutchison JL, Hubbard NA, Brigante RM, Turner M, Sandoval TI, Hillis GAJ, et al. The efficiency
762 of fMRI region of interest analysis methods for detecting group differences. J Neurosci
763 Methods. 2014;226:57–65. doi: 10.1016/j.jneumeth.2014.01.012

764 34. Geuter S, Boll S, Eippert F, Büchel C. Functional dissociation of stimulus intensity encoding and
765 predictive coding of pain in the insula. Elife. 2017;6. doi: 10.7554/eLife.24770

766 35. Moayedi M, Weissman-Fogel I. Is the insula the "how much" intensity coder? J Neurophysiol.
767 2009;102(3):1345–7. doi: 10.1152/jn.00356.2009

768 36. Berret E, Kintscher M, Palchaudhuri S, Tang W, Osypenko D, Kochubey O, et al. Insular cortex
769 processes aversive somatosensory information and is crucial for threat learning. Science (80-
770). 2019;eaaw0474. doi: 10.1126/science.aaw0474

771 37. Taylor KS, Seminowicz DA, Davis KD. Two systems of resting state connectivity between the
772 insula and cingulate cortex. Hum Brain Mapp. 2009;30(9):2731–45. doi: 10.1002/hbm.20705

38. Eckert MA, Menon V, Walczak A, Ahlstrom J, Denslow S, Horwitz A, et al. At the heart of the ventral attention system: the right anterior insula. Hum Brain Mapp. 2009;30(8):2530–41. doi: 10.1002/hbm.20688

39. Mazzola L, Isnard J, Peyron R, Mauguière F. Stimulation of the human cortex and the experience of pain: Wilder Penfield's observations revisited. Brain. 2012;135(2):631–40. doi: 10.1093/brain/awr265

40. Mazzola L, Faillenot I, Barral F-G, Mauguière F, Peyron R. Spatial segregation of somato-sensory and pain activations in the human operculo-insular cortex. Neuroimage. 2012;60(1):409–18. doi: 10.1016/j.neuroimage.2011.12.072

41. Ostrowsky K, Magnin M, Ryvlin P, Isnard J, Guenot M, Mauguière F. Representation of pain and somatic sensation in the human insula: a study of responses to direct electrical cortical stimulation. Cereb Cortex. 2002;12(4):376–85.

42. Garcia-Larrea L, Mauguière F. Pain syndromes and the parietal lobe. In: Handbook of Clinical Neurology. 2018. p. 207–23. doi: 10.1016/B978-0-444-63622-5.00010-3

43. Liang M, Su Q, Mouraux A, Iannetti GD. Spatial Patterns of Brain Activity Preferentially Reflecting Transient Pain and Stimulus Intensity. Cereb Cortex. 2019;29(5):2211–27. doi: 10.1093/cercor/bhz026

44. Baliki MN, Geha PY, Fields HL, Apkarian AV. Predicting value of pain and analgesia: Nucleus accumbens response to noxious stimuli changes in the presence of chronic pain. Neuron. 2010;66(1):149–60. doi: 10.1016/j.neuron.2010.03.002

45. Xia C, Touroutoglou A, Quigley KS, Feldman Barrett L, Dickerson BC. Salience Network Connectivity Modulates Skin Conductance Responses in Predicting Arousal Experience. J Cogn Neurosci. 2017;29(5):827–36. doi: 10.1162/jocn_a_01087

46. Price DD, McGrath PA, Rafii A, Buckingham B. The validation of visual analogue scales as ratio

797 scale measures for chronic and experimental pain. Pain. 1983;17(1):45–56. doi:
798 10.1016/0304-3959(83)90126-4

799 47. Duncan GH, Bushnell CM, Lavigne GJ. Comparison of verbal and visual analogue scales for
800 measuring the intensity and unpleasantness of experimental pain. Pain. 1989;37(3):295–303.
801 doi: 10.1016/0304-3959(89)90194-2

802 48. Quiton RL, Greenspan JD. Across- and within-session variability of ratings of painful contact
803 heat stimuli. Pain. 2008;137(2):245–56. doi: 10.1016/j.pain.2007.08.034

804 49. Lashkari D, Vul E, Kanwisher N, Golland P. Discovering structure in the space of fMRI
805 selectivity profiles. Neuroimage. 2010;50(3):1085–98. doi: 10.1016/j.neuroimage.2009.12.106

806 50. Kanwisher N. Functional specificity in the human brain: A window into the functional
807 architecture of the mind. Proc Natl Acad Sci. 2010;107(25):11163–70. doi:
808 10.1073/pnas.1005062107

809 51. Beck AT, Steer RA, Brown GK. Manual for the Beck Depression Inventory-II. San Antonio, TX:
810 Psychological Corporation Press; 1996.

811 52. Kroenke K, Spitzer RL, Williams JBW. The PHQ-15: validity of a new measure for evaluating the
812 severity of somatic symptoms. Psychosom Med. 2002;64(2):258–66.

813 53. Benedek M, Kaernbach C. A continuous measure of phasic electrodermal activity. J Neurosci
814 Methods. 2010;190(1):80–91. doi: 10.1016/J.JNEUMETH.2010.04.028

815 54. Geuter S, Gamer M, Onat S, Büchel C. Parametric trial-by-trial prediction of pain by easily
816 available physiological measures. Pain. 2014;155(5):994–1001. doi:
817 10.1016/j.pain.2014.02.005

818 55. Loggia ML, Juneau M, Bushnell MC. Autonomic responses to heat pain: Heart rate, skin
819 conductance, and their relation to verbal ratings and stimulus intensity. Pain.
820 2011;152(3):592–8. doi: 10.1016/j.pain.2010.11.032

821 56. Bach DR, Flandin G, Friston KJ, Dolan RJ. Modelling event-related skin conductance responses.
822 Int J Psychophysiol. 2010;75(3):349–56. doi: 10.1016/J.IJPSYCHO.2010.01.005

823 57. Eickhoff SB, Stephan KE, Mohlberg H, Grefkes C, Fink GR, Amunts K, et al. A new SPM toolbox
824 for combining probabilistic cytoarchitectonic maps and functional imaging data. Neuroimage.
825 2005;25(4):1325–35. doi: 10.1016/J.NEUROIMAGE.2004.12.034

826 58. Rolke R, Magerl W, Campbell KA, Schalber C, Caspari S, Birklein F, et al. Quantitative sensory
827 testing: A comprehensive protocol for clinical trials. Eur J Pain. 2006;10(1):77–88. doi:
828 10.1016/j.ejpain.2005.02.003

829 59. Ellerbrock I, May A. MRI scanner environment increases pain perception in a standardized
830 nociceptive paradigm. Brain Imaging Behav. 2015;9(4):848–53. doi: 10.1007/s11682-014-
831 9345-5

832 60. Awiszus F. TMS and threshold hunting. Suppl Clin Neurophysiol. 2003;56:13–23. doi:
833 10.1016/S1567-424X(09)70205-3

834 61. Hall DA, Summerfield AQ, Gonçalves MS, Foster JR, Palmer AR, Bowtell RW. Time-course of
835 the auditory BOLD response to scanner noise. Magn Reson Med. 2000;43(4):601–6.

836 62. National Institute for Occupational Health and Safety (NIOSH). Criteria for a Recommended
837 Standard: Occupational Noise Exposure. Revised Criteria [Internet]. 1998.

838 63. Kass RE, Raftery AE. Bayes Factors. J Am Stat Assoc. 1995;90(430):773–95. doi:
839 10.1080/01621459.1995.10476572

840 64. Rouder JN, Morey RD. Default Bayes Factors for model selection in regression. Multivariate
841 Behav Res. 2012;47(6):877–903. doi: 10.1080/00273171.2012.734737

842 65. Raudenbush SW, Bryk AS. Hierarchical linear models: Applications and data analysis.
843 Thousand Oaks, CA: Sage; 2002.

66. Hofmann DA, Gavin MB. Centering decisions in Hierarchical Linear Models: Implications for research in organizations. J Manage. 1998;24(5):623–41. doi: 10.1177/014920639802400504

847 ## Supporting information

848

849 **S1 Tab**. Sample descriptive statistics.

Questionnaire	Construct	Mean±SD	Sample range	Possible range
BDI-II [SR 1,2]	Depression	2.0±2.2	0-8	0-63
PHQ15 [SR 3]	Somatization	3.9±2.3	0-9	0-30
FPQ [SR 4]				
severe	Fear of pain	28.9±8.3	11-42	10-50
minor	Fear of pain	14.0±4.5	10-27	10-50
PVAQ [SR 5]	Pain vigilance and awareness	34.6±8.7	21-54	0-80
PSQ [SR 6]	Pain sensitivity	45.1±14.8	17-73	0-140
PRSS [SR 7]				
Catastrophizing	Pain catastrophizing	8.6±5.4	2-21	0-45, higher more catastrophizing
Coping	Pain coping	29.8±5.2	19-38	0-45, higher more active coping
STAI [SR 8,9]				
Trait	Trait anxiety	32.0±6.9	21-49	20-80
State	State anxiety (pre experiment)	31.5±6.2	22-51	20-80
MDMQ [SR 10]				
GoodBad A	Mood: Good vs bad (pre exp.)	17.7±1.9	12-20	4-24, the higher the better
AwakeTired A	Mood: Awake vs tired (pre exp.)	15.2±2.9	8-19	4-24, the higher the more awake

CalmNervous A	Mood: Calm vs nervous (post exp.)	16.5±2.6	10-20	4-24, the higher the calmer
GoodBad B	Mood: Good vs bad (pre exp.)	17.2±1.7	12-19	4-24, the higher the better
AwakeTired B	Mood: Awake vs tired (pre exp.)	10.1±2.4	6-16	4-24, the higher the more awake
CalmNervous B	Mood: Calm vs nervous (post exp.)	17.2±2.1	12-20	4-24, the higher the calmer

852 **S2 Tab**. Average calibrated sound intensities 1 through 6, which were used as stimuli during the experiment.

853 Cohort 2 received higher intensities, see Materials and Methods for rationale.

	Cohort 1 (n=15)			**Cohort 2 (n=11)**		
Intensity	**Target VAS**	**dBA mean±SD**	**Range**	**Target VAS**	**dBA mean±SD**	**Range**
1	25	73.3±5.4	61.0-82.9	48	85.0±9.0	65.7-99.3
2	35	77.0±4.9	67.7-85.9	59	91.3±8.3	71.1-101.5
3	45	80.5±5.0	73.6-89.6	70	95.1±7.6	76.3-102.5
4	55	83.8±5.4	76.7-96.1	82	97.6±6.1	81.7-103.0
5	65	86.6±5.4	78.9-99.3	93	99.3±4.8	86.3-103.0
6	75	89.1±5.2	81.0-100.5	105	100.6±3.5	91.0-103.0

854

855

856 **S3 Tab.** Differences of behavioral and psychological measures of the SCR-selected subsample compared to the

857 not-selected subsample.

Measure	Mean±SD of n=26 included subjects[1]	Mean±SD of n=32 excluded subjects	Mean differences[2]	Variance differences[3]
Heat pain threshold	43.5±1.1	43.3±1.1	t(56)=0.496, p=0.622	F(31,25)=1.000, p=0.989
Heat intensity 1	41.9±1.4	41.7±1.4	t(56)=0.499, p=0.620	F(31,25)=1.094, p=0.825
Heat intensity 2	42.5±1.3	42.3±1.2	t(56)=0.508, p=0.613	F(31,25)=1.066, p=0.879
Heat intensity 3	43.1±1.1	43.0±1.1	t(56)=0.505, p=0.615	F(31,25)=1.024, p=0.961
Heat intensity 4	43.8±1.0	43.7±1.0	t(56)=0.480, p=0.633	F(31,25)=0.975, p=0.936
Heat intensity 5	44.4±1.0	44.3±1.0	t(56)=0.424, p=0.673	F(31,25)=0.930, p=0.840
Heat intensity 6	45.1±1.0	45.0±1.1	t(56)=0.343, p=0.733	F(31,25)=0.905, p=0.785
Sound unpleasantness threshold	82.9±7.3	83.9±7.0	t(56)=-0.537, p=0.593	F(31,25)=1.079, p=0.853
Sound intensity 1	76.8±10.4	78.3±9.2	t(56)=-0.552, p=0.583	F(31,25)=1.283, p=0.528
Sound intensity 2	81.9±9.9	83.1±9.6	t(56)=-0.454, p=0.651	F(31,25)=1.063, p=0.885
Sound intensity 3	86.2±9.8	86.7±9.5	t(56)=-0.206, p=0.838	F(31,25)=1.055, p=0.901
Sound intensity 4	89.6±9.1	89.6±8.9	t(56)=-0.004, p=0.997	F(31,25)=1.041, p=0.928
Sound intensity 5	92.4±8.0	92.0±8.1	t(56)=0.172, p=0.864	F(31,25)=0.973, p=0.932
Sound intensity 6	94.7±6.9	94.0±7.3	t(56)=0.369, p=0.714	F(31,25)=0.899, p=0.771

858 [1]Included subjects pooled over both cohorts; [2]Two-sample t-test; [3]Two-sample F-test

859

860

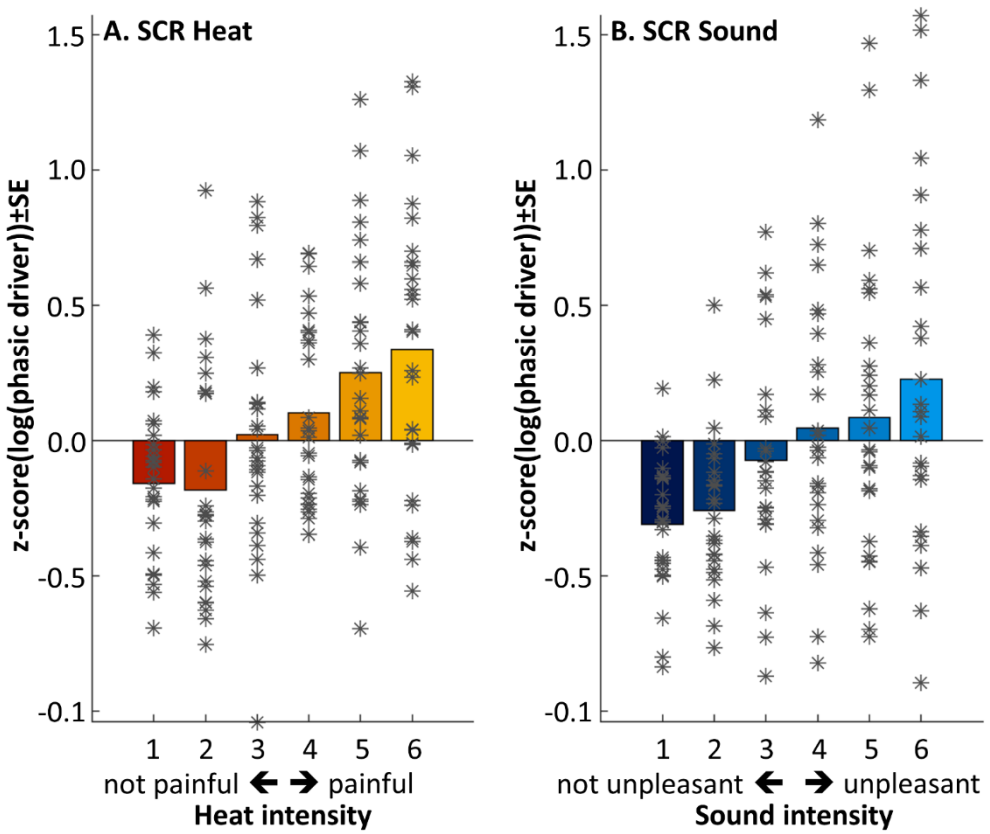

S1 Fig. Skin conductance responses following heat (**A**) and sound stimuli (**B**), with individual data points. The pain and unpleasantness thresholds were located between intensities 3 and 4, as per calibration.

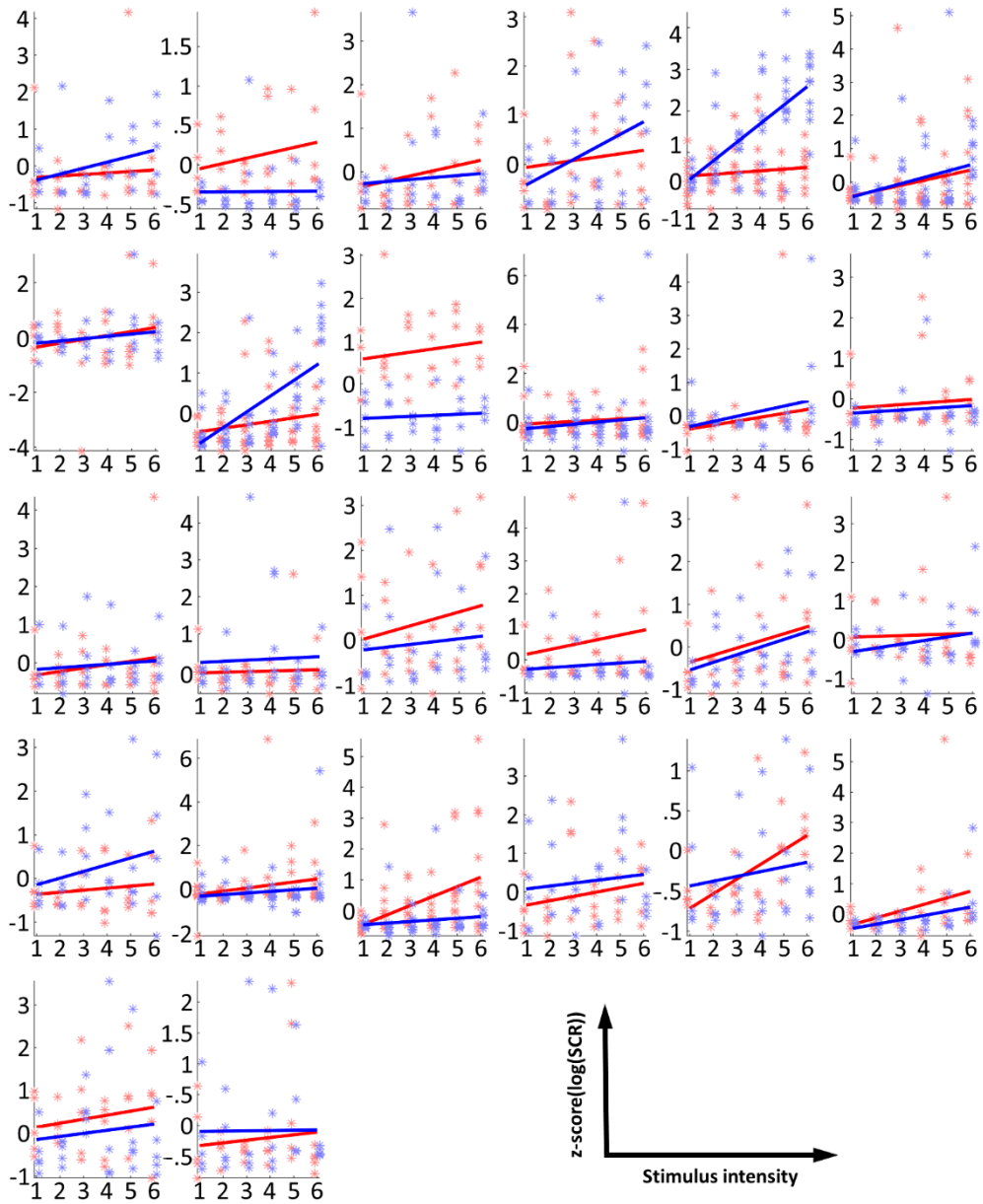

S2 Fig. Single subject skin conductance responses following heat (red) and sound stimuli (blue). Asterisks indicate single responses, lines are regression curves as per linear regression. The pain and unpleasantness thresholds were located between intensities 3 and 4, as per calibration.

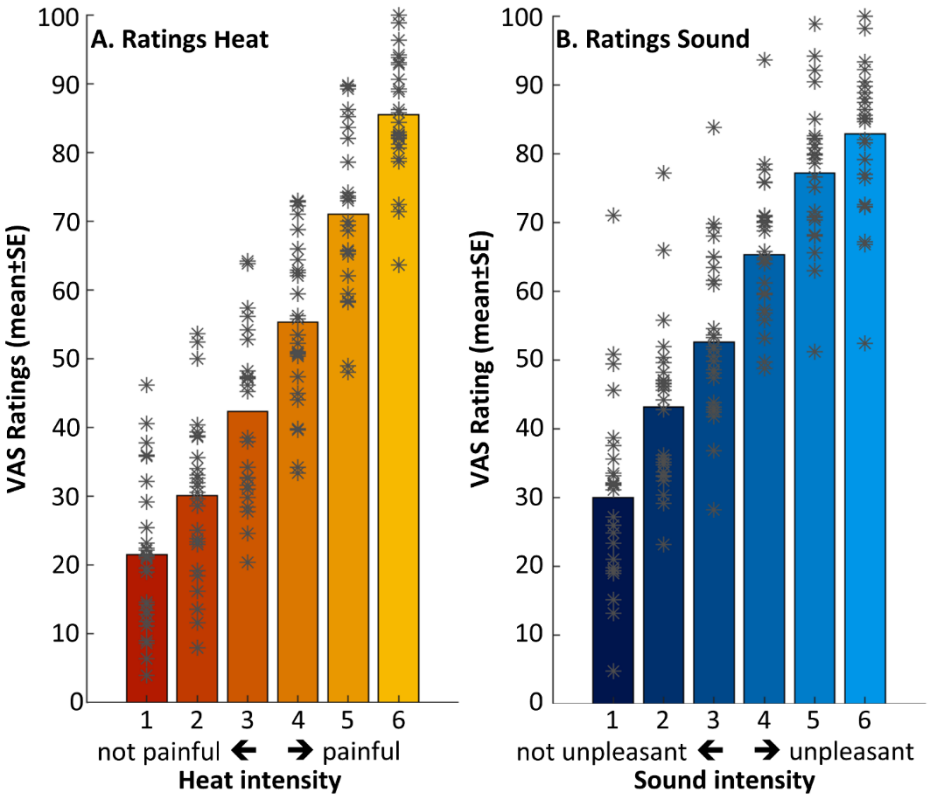

S3 Fig. Behavioral ratings following heat (**A**) and sound stimuli (**B**), with individual data points. The pain and unpleasantness thresholds were located between intensities 3 and 4, as per calibration.

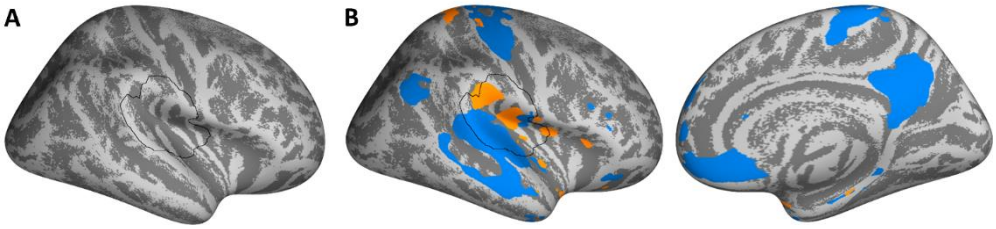

S4 Fig. Binary and signed masks used for analyses. **A.** Binary mask used for small volume correction used for all analyses (unless otherwise noted), delineated by the black line. **B.** Signed mask used for covering heat (orange) or sound (blue) contrasts.

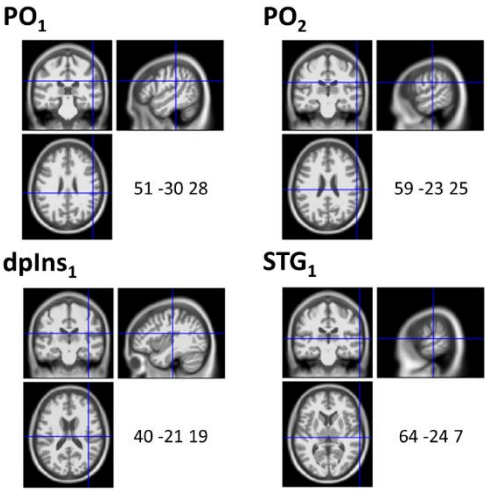

S5 Fig. Location of peak voxels for modality main effects in the parietal operculum (PO_1, PO_2) and dorsal posterior insula ($dpIns_1$) for heat, superior temporal gyrus (STG_1) for sound. Also see Fig 4.

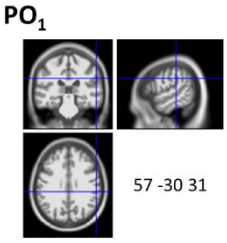

S6 Fig. Location of peak voxel for parametric modulation by heat intensity in the parietal operculum (PO_1). Also see Fig 5.

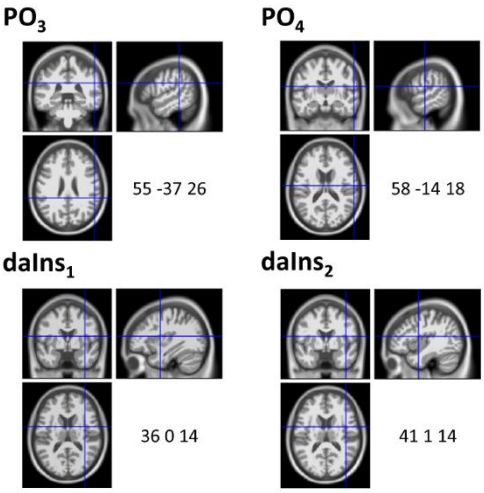

S7 Fig. Location of peak voxels for parametric modulation by ratings in the parietal operculum (PO_3, PO_4) and dorsal anterior insula ($daIns_1$, $daIns_2$). Also see Fig 6.

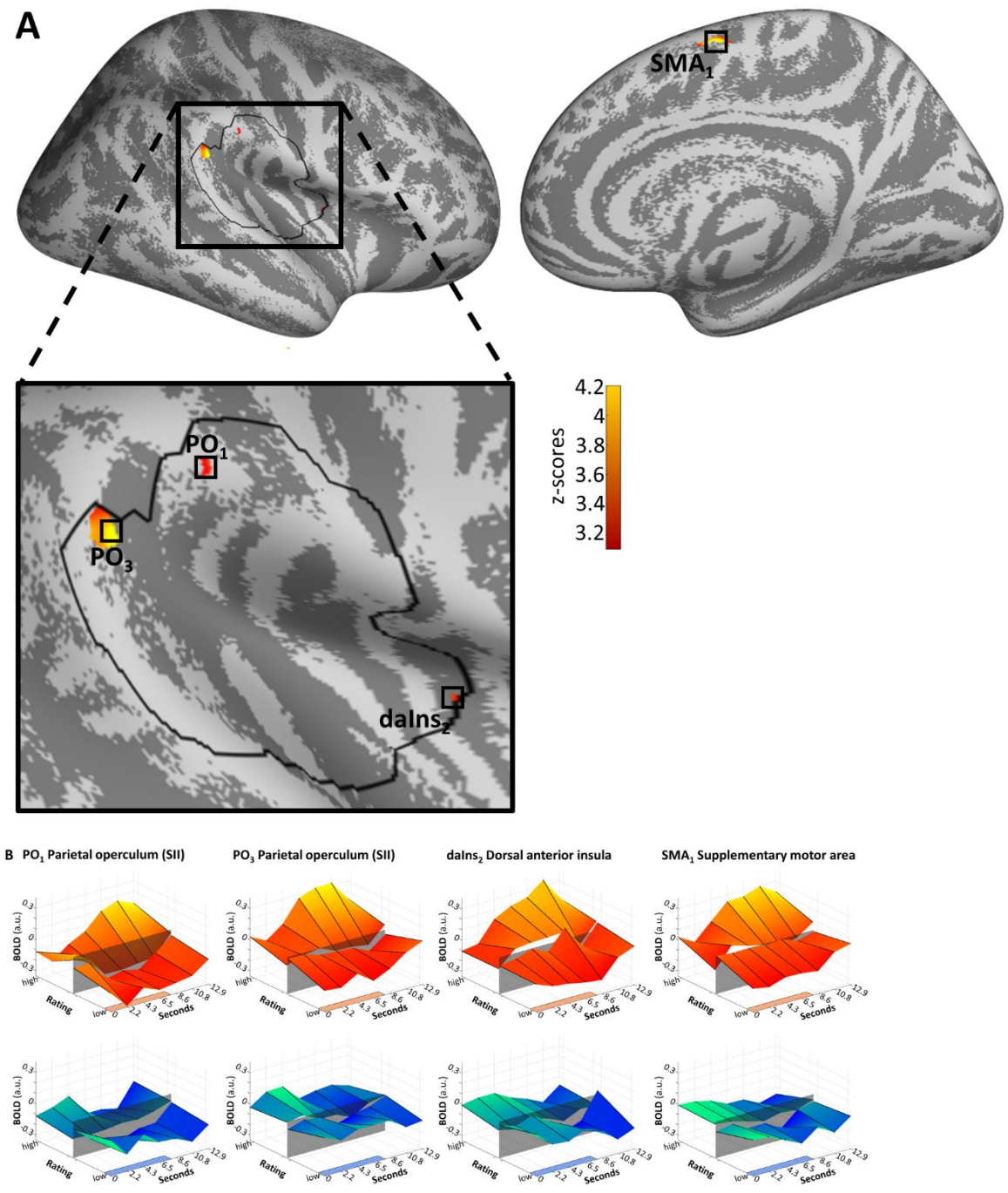

S8 Fig. Medial surface view for areas that fulfill the axiomatic requirements of differential activation during pain compared to heat and sound (also see Fig 7). Unlike in Fig 7, activations are shown after analysis with a lower threshold of p(uncorrected)<0.001. At this threshold, activation was found in the parietal operculum (PO_3 is the cluster reported in Fig 7; PO_1 is a more dorsal cluster), the dorsal anterior insula ($daIns_2$) and the (pre-)supplementary motor area (SMA_1). Exact coordinates and activation of cluster peaks were x=55, y=-37, z=24, Z=4.176, p(uncorrected)=1e-05 (PO_3), x=61, y=-26, z=30, Z=3.26, p(uncorrected)=6e-04 (PO_1), x=35, y=1, z=13, Z=3.297, p(uncorrected)=5e-04 ($daIns_2$), and x=7, y=-5, z=60, Z=4.202, p(uncorrected)=1e-05 (SMA_1). **A**.

Activations are thresholded at p(uncorrected)<0.001 and overlaid on an average brain surface. The black line delineates the SVC mask. **B**. Poststimulus plots of fMRI activation in the four vertices during heat (orange) and sound (blue). The shaded patch in the center signifies the pain threshold (for heat) and unpleasantness threshold (for sound). The colored patches at the right axes show the stimulus duration.

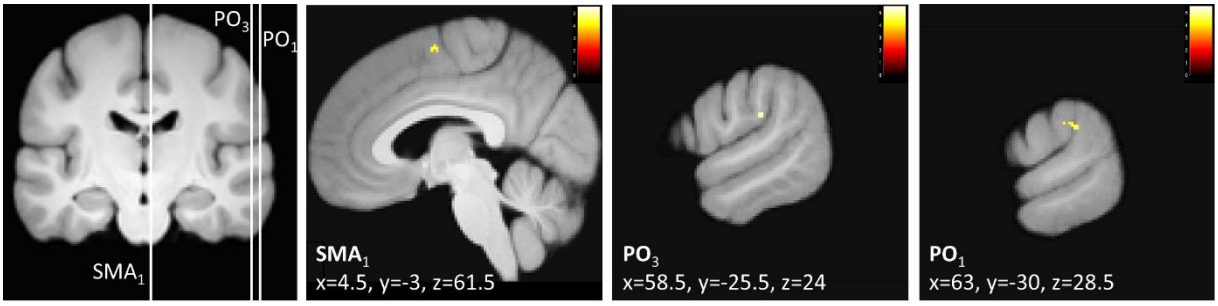

S9 Fig. Conventional 3D analysis for areas that fulfill the axiomatic requirements of differential activation during pain compared to heat and sound (also see Fig 7). No activations were significant at our predefined threshold (p<0.05, corrected). For reasons of completeness, this analysis is reported at a lower threshold of p(uncorrected)<0.001. The location of activations roughly correspond to the surface analysis presented in S8 Fig. Activation was observed in the parietal operculum (PO_3 is the cluster reported in Fig 7; PO_1 is a more dorsal cluster) and the (pre-)supplementary motor area (SMA_1), among other areas. Exact coordinates and activation of cluster peaks were x=59, y=-26, z=24, Z=3.9, p(uncorrected)=5e-05 (PO_3), x=63, y=-30, z=29, Z=3.487, p(uncorrected)=2e-04 (PO_1), and x=5, y=3, z=62, Z=3.297, p(uncorrected)=3e-04 (SMA_1). Activations are thresholded at p(uncorrected)<0.001 and overlaid on an average brain.

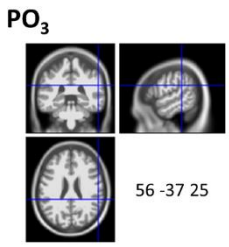

S10 Fig. Location of peak voxel for activation corresponding to the four axioms in the parietal operculum (PO_3). Also see Fig 7.

921

Supporting information – References

SR 1. Beck AT, Steer RA, Brown GK. Manual for the Beck Depression Inventory-II. San Antonio, TX: Psychological Corporation Press; 1996.

SR 2. Hautzinger M, Keller F, Kühner C. BDI-II. Beck-Depressions-Inventar. Revision. 2nd ed. Frankfurt: Pearson Assessment; 2009.

SR 3. Kroenke K, Spitzer RL, Williams JBW. The PHQ-15: validity of a new measure for evaluating the severity of somatic symptoms. Psychosom Med. 2002;64(2):258–66.

SR 4. McNeil DW, Rainwater AJ. Development of the Fear of Pain Questionnaire-III. J Behav Med. 1998;21(4):389–410.

SR 5. McCracken LM. “Attention” to pain in persons with chronic pain: A behavioral approach. Behav Ther. 1997;28(2):271–84. doi: 10.1016/S0005-7894(97)80047-0

SR 6. Ruscheweyh R, Marziniak M, Stumpenhorst F, Reinholz J, Knecht S. Pain sensitivity can be assessed by self-rating: Development and validation of the Pain Sensitivity Questionnaire. Pain. 2009;146(1):65–74. doi: 10.1016/j.pain.2009.06.020

SR 7. Flor H, Behle DJ, Birbaumer N. Assessment of pain-related cognitions in chronic pain patients. Behav Res Ther. 1993;31(1):63–73.

SR 8. Spielberger CD, Gorsuch RL, Lushene RE. Manual for the State-Trait Anxiety Inventory. Palo Alto, CA: Consulting Psychologists Press; 1970.

SR 9. Laux L, Glanzmann P, Schaffner P, Spielberger CD. Das State-Trait-Angstinventar. Weinheim: Beltz; 1981.

SR 10. Steyer R, Schwenkmezger P, Notz P, Eid M. Der Mehrdimensionale Befindlichkeitsfragebogen (MDBF). Handanweisung. Göttingen: Hogrefe; 1997.